Atmos. Chem. Phys. Discuss., 14, 2717–2771, 2014
www.atmos-chem-phys-discuss.net/14/2717/2014/
doi:10.5194/acpd-14-2717-2014

Atmospheric
Chemistry
and Physics
Discussions
Open Access

Re-evaluating the reactive uptake of HOBr in the troposphere with implications for the marine boundary layer and volcanic plumes

T. J. Roberts[1], **L. Jourdain**[1], **P. T. Griffiths**[2], **and M. Pirre**[1]

[1] LPC2E, UMR7328, CNRS-Université d'Orléans, 3A Avenue de la Recherche Scientifique, 45071 Orleans, Cedex 2, France
[2] Centre for Atmospheric Science, Cambridge University, Chemistry Department, Lensfield Road, Cambridge, CB2 1EW, UK

Received: 15 November 2013 – Accepted: 3 December 2013 – Published: 27 January 2014

Correspondence to: T. J. Roberts (tjarda.roberts@crns-orleans.fr)

Published by Copernicus Publications on behalf of the European Geosciences Union.

Abstract

The reactive uptake of HOBr onto halogen-rich aerosols promotes conversion of $Br^-_{(aq)}$ into gaseous reactive bromine (incl. BrO) with impacts on tropospheric oxidants and mercury deposition. However, experimental data quantifying HOBr reactive uptake on tropospheric aerosols is limited, and reported values vary in magnitude. This study re-examines the reaction kinetics of HOBr across a range of aerosol acidity conditions, focusing on chemistry within the marine boundary layer and volcanic plumes.

We highlight that the termolecular approach to HOBr reaction kinetics, used in numerical model studies to date, is strictly only valid over a specific pH range. Here we re-evaluate the reaction kinetics of HOBr according to the general acid assisted mechanism. The rate of reaction of HOBr with halide ions becomes independent of pH at high acidity yielding an acid-independent second-order rate constant, k^{II}. The limit of acid-saturation is poorly constrained by available experimental data, although a reported estimate for $HOBr + Br^-_{(aq)} + H^+_{(aq)}$, is $k^{II}_{sat} = 10^8$–$10^9\ M^{-1}\ s^{-1}$, at pH $\lesssim 1$. By consideration of halide nucleophilic strength and re-evaluation of reported uptake coefficient data on H_2SO_4-acidified sea-salt aerosol, we suggest the reaction of $HOBr_{(aq)} + Cl^-_{(aq)} + H^+_{(aq)}$ may saturate to become acid-independent at pH ≤ 6, with $k^{II}_{sat} \sim 10^4\ M^{-1}\ s^{-1}$. This rate constant is multiple orders of magnitude lower (a factor of 10^3 at pH = 3 and a factor of 10^6 at pH = 0) than that currently assumed in numerical models of tropospheric BrO chemistry, which are based on the termolecular approach.

Reactive uptake coefficients, γ_{HOBr}, were calculated as a function of composition using the revised HOBr kinetics, with $k^I = k^{II} \cdot [X^-_{(aq)}]$, and X = Br or Cl. γ_{HOBr} initially increases with acidity but subsequently declines with increasing H_2SO_4-acidification of sea-salt aerosol. The $HOBr + Cl^-$ uptake coefficient declines due to acid-displacement of $HCl_{(g)}$, reducing $[Cl^-_{(aq)}]$. The $HOBr+Br^-$ uptake coefficient also declines at very high H_2SO_4 : Na ratios due to dilution of $[Br^-_{(aq)}]$. The greatest reductions in HOBr uptake coefficients occur for small particle sizes, across which the probability of diffusion of

$HOBr_{(aq)}$ without reaction is highest. Our new uptake calculations are consistent with all reported experimental data thus resolve previously reported discrepancies within a unified uptake coefficient framework.

The following implications for BrO chemistry in the marine boundary layer are highlighted: we confirm HOBr reactive uptake is rapid on moderately acidified supramicron aerosol, but predict very low HOBr reactive uptake coefficients on the highly-acidified submicron marine aerosol fraction. This re-evaluation is in contrast to the high HOBr reactive uptake previously assumed to occur on all acidified sea-salt aerosol. Instead, our uptake evaluation indicates that particle bromide in the submicron aerosol fraction is not easily depleted by HOBr uptake, and furthermore can be augmented by deposition of gas-phase bromine released from the supramicron particles. We present this mechanism as a first explanation for the observed (but previously unexplained) Br-enhancement (relative to Na) in submicron particles in the marine environment. Further, we find HOBr reactive uptake on acidified sea-salt aerosol is driven by reaction of $HOBr + Br^-$ rather than $HOBr + Cl^-$ ($\gamma_{HOBr+Br-} > \gamma_{HOBr^-+Cl^-}$) once HCl-displacement has occurred. Thus, the reduction in $\gamma_{HOBr+Br^-}$ as BrO chemistry progresses (noting $\gamma_{HOBr+Br^-}$ is a function of aerosol $Br^-_{(aq)}$ concentration which declines as aerosol bromide is converted into gaseous-phase reactive bromine) will have greater importance in slowing overall HOBr reactive uptake as BrO chemistry evolves than has been assumed previously. We suggest both the above factors may explain the reported over-prediction of BrO cycling in the marine environment by numerical models to date.

First predictions of HOBr reactive uptake on sulphate particles in tropospheric volcanic plumes are presented. High (accommodation limited) $HOBr + Br^-$ uptake coefficient in concentrated (> 1 ppmv SO_2) plume environments supports rapid BrO formation under all conditions. However, the $HOBr + Cl^-$ uptake coefficient exhibits an inverse temperature trend which becomes more pronounced as the plume disperses. The $HOBr + Br^-$ coefficient also declines with temperature in dilute (~ ppbv SO_2) plumes. We infer that BrO chemistry can readily be sustained in downwind plumes entering the mid- to-upper troposphere, e.g. either from continuous degassing from elevated volcano summits (e.g. Etna, 3.3 km a.s.l.) or episodic eruptions (e.g. Eyjafjallajökull, Iceland). However, low HOBr reactive uptake coefficients may limit sustained BrO cycling in dilute plumes in the lower troposphere.

In summary, our revised HOBr kinetics that includes acid-saturation indicates that current numerical models of BrO chemistry in the troposphere substantially overestimate the rate of HOBr reactive uptake on acidic halogen rich-particles, with implications for BrO chemistry in both the marine environment and volcanic plumes, as well as the wider troposphere.

1 Introduction

The reactive uptake of HOBr onto halogen-containing aerosols to release Br_2 enables propagation of the chain reaction leading to autocatalytic BrO formation, the so-called "bromine explosion", (Vogt et al., 1996), first proposed following the discovery of ozone depletion events in the polar boundary layer (Barrie et al., 1988). Rapid and substantial (10's ppbv) ozone depletion occurs upon the formation of just 10's pptv BrO due to cycling between Br and BrO, with further Br-mediated impacts on environmental mercury in the conversion of Hg^0 to more reactive and easily deposited form Hg^{II} (Schroeder et al., 1998). Tropospheric BrO chemistry has since been recognised outside the polar regions, with BrO identified above salt pans (Hebestreit et al., 1999), in the marine boundary layer (Read et al., 2008), and is suggested to have a significant impact on the chemistry of the free troposphere (e.g. von Glasow et al., 2004). In particular, recent evidence of rapid BrO formation in acidic volcanic plumes (10's pptv to ppbv on a timescale of minutes) has highlighted volcanic halogen emissions as a source of reactive bromine entering the troposphere (Bobrowski et al., 2003).

To this respect, numerical models have been developed to better understand the formation of BrO and evaluate impacts on atmospheric oxidants throughout the troposphere and on mercury cycling in the environment. For the different tropospheric environments, the models capture the salient features of BrO formation and impacts (e.g.

on ozone depletion and Hg deposition events), for example see reviews by Simpson et al. (2007) and Saiz-Lopez and von Glasow (2012) and references therein. Nevertheless, a number of uncertainties remain. For example, models tend to overestimate Br_x cycling in the marine environment (Sander et al., 2003; Smoydzin and von Glasow, 2007; Keene et al., 2009). Models predict a depletion in the inorganic bromine content of all acidified marine aerosols, as consequence of HOBr reactive uptake to form Br_2 and its release into the gas-phase. However, an aerosol bromine deficit is only observed in the slightly acidified supramicron fraction, whilst aerosol bromine is found to be enhanced (relative to that expected based on Br : Na ratios in sea-salt, using sodium as a sea-salt tracer) in the highly acidified sub-micronmeter fraction. This phenomenon has not been explained to date (Sander et al., 2003). Numerical models have also attempted to simulate reactive halogen chemistry in volcanic plume environments. Models initialised with a high-temperature source region, are able to reproduce the rapid formation of BrO in the near-source plume (Bobrowski et al., 2007a; Roberts et al., 2009; Von Glasow, 2010), as well as ozone depletion (Kelly et al., 2013), but a source of model uncertainty is the representation of heterogeneous halogen chemistry on volcanic aerosol, which may differ from that reported from experiments on sea-salt aerosol.

All these studies rely on laboratory experiments to quantify rate constants of the reactions, with a key process in the formation of reactive bromine being the reaction of $HOBr_{(aq)}$ with halide ion $X^-_{(aq)}$ ($Cl^-_{(aq)}$ or $Br^-_{(aq)}$) and $H^+_{(aq)}$.

$$HOBr_{(aq)} + H^+_{(aq)} + X^-_{(aq)} \xrightarrow{k_{ter},\ k^{II},\ k^{I}} BrX_{(aq)} + H_2O_{(aq)} \tag{R1}$$

Experimental studies (e.g. Fickert et al., 1999) show the reaction of $HOBr_{(aq)}$ is promoted when alkaline sea-salt aerosols becomes acidified, either by natural (e.g. methane sulphonic acid) or anthropogenic (e.g. sulphuric acid) sources of acidity. However, laboratory experiments have reported uptake coefficients on acidified sea-salt aerosol, > 0.2 (Abbatt and Wachewsky, 1998) and 10^{-2} (Pratte and Rossi, 2006), a discrepancy that has not been explained to date. In addition, no experiments have been performed to quantify uptake of HOBr on volcanic aerosol under tropospheric conditions.

Numerical model studies of reactive bromine chemistry currently implement Reaction (R1) using three-body reaction kinetics, i.e. assumed the reaction rate is directly proportional to $H^+_{(aq)}$ concentration (e.g. von Glasow, 2002), or using uptake coefficients calculated on this assumption (IUPAC evaluations, e.g. Ammann et al., 2013). We highlight, however, that earlier literature on the general acid-assisted mechanism for this and similar reactions (e.g. Eigen and Kustin, 1962; Nagy et al., 1988) identify that the pH dependence of the reaction rate is more complex, with acid-saturation of the kinetics at high acidity.

This study re-evaluates HOBr reactive uptake in the context of the general acid assisted mechanism for the first time. First we evaluate the second-order rate constants for the reaction of $HOBr + Br^-$ and $HOBr + Cl^-$ from reported literature data with use of a thermodynamic model to predict aerosol composition under experimental conditions. Secondly, we evaluate the uptake coefficients for HOBr onto HCl-acidified and H_2SO_4-acidified aerosol. We provide new quantification of $HOBr + Br^-$ and $HOBr + Cl^-$ uptake coefficients on H_2SO_4-acidified sea-salt aerosol in the marine environment, and sulphuric acid aerosol in volcanic plumes dispersing into the troposphere. Implications for our understanding of reactive halogen chemistry in the troposphere and improvements to numerical modelling are discussed.

2 The reactive uptake of HOBr

2.1 Reactive bromine chemistry in the troposphere

Reactions (R2)–(R11) illustrate the autocatalytic mechanism for BrO formation in the troposphere, in the so-called “bromine explosion”. The mechanism requires halogens, aerosol and sunlight to be present, and acts to convert $Br^-_{(aq)}$ (or HBr) into reactive bromine (that includes BrO, HOBr, $BrONO_2$, $BrNO_2$, Br_2, BrCl, Br). The reaction of

HOBr with $X^-_{(aq)}$ in the aerosol phase is a key step in the propagation of the reaction cycles and the release of reactive halogens to the gas-phase.

$$HOBr_{(g)} \rightarrow HOBr_{(aq)} \tag{R2}$$

$$HOBr_{(aq)} + Br^-_{(aq)} + H^+_{(aq)} \rightarrow Br_{2\,(aq)} + H_2O_{(l)} \tag{R3}$$

$$HOBr_{(aq)} + Cl^-_{(aq)} + H^+_{(aq)} \rightarrow BrCl_{(aq)} + H_2O_{(l)} \tag{R4}$$

$$BrCl_{(aq)} + Br^-_{(aq)} \leftrightarrow Br_2Cl^-_{(aq)} \leftrightarrow Br_{2\,(aq)} + Cl^-_{(aq)} \tag{R5}$$

$$Br_{2\,(aq)} \leftrightarrow Br_{2\,(g)} \tag{R6}$$

$$Br_{2\,(g)} \xrightarrow{h\nu} 2Br_{(g)} \tag{R7}$$

$$2Br_{(g)} + 2O_{3\,(g)} \rightarrow 2BrO_{(g)} + 2O_{2\,(g)} \tag{R8}$$

$$2BrO_{(g)} \rightarrow 2Br_{(g)} + O_{2\,(g)} \tag{R9}$$

$$2BrO_{(g)} \rightarrow Br_{2\,(g)} + O_{2\,(g)} \tag{R10}$$

$$2BrO_{(g)} + 2HO_{2\,(g)} \rightarrow 2HOBr_{(g)} + 2O_{2\,(g)} \tag{R11}$$

The reactive uptake of HOBr involves accommodation of $HOBr_{(g)}$ to aerosol and reaction with $Cl^-_{(aq)}$ or $Br^-_{(aq)}$ to form $BrCl_{(aq)}$ or $Br_{2\,(aq)}$, Reactions (R2)–(R4). The reaction of HOBr with $Cl^-_{(aq)}$ (Reaction R4) is typically considered the dominant reaction pathway (albeit an assumption that may not apply in highly acidified aerosol as we show in this study) given sea-salt aerosol contains $[Br^-_{(aq)}] \ll [Cl^-_{(aq)}]$ by a factor of 700 (or greater once reactive bromine formation has commenced), and the termolecular rate constants for Reactions (R3) and (R4) are of comparable magnitudes (Liu and Margarem, 2001; Beckwith et al., 1996). However, Br_2 is commonly the observed product, as confirmed by laboratory experiments by Fickert et al. (1999). The product conversion from BrCl to Br_2 is explained by aqueous-phase equilibria (Reaction R5) that interconvert BrCl into Br_2 (via Br_2Cl^-) before gaseous release (Reaction R6). According to equilibrium constants reported by Wang et al. (1994), conversion of BrCl to Br_2 is favoured at room temperature in aerosol provided $Br^-_{(aq)} : Cl^-_{(aq)} \gtrsim 10^{-4}$, as for example in sea-salt aerosol where $Br^-_{(aq)} : Cl^-_{(aq)} \approx 1.5 \times 10^{-3}$. The dihalogen species then partition into the gas-phase, Reaction (R6). The exsolution of dihalogens from the aerosol to the gas-phase also limits the occurrence of reverse reactions that might reform HOBr. Once in the gas-phase, Br_2 is photolysed to produce 2 Br radicals, Reaction (R7), which may react with ozone to form BrO, Reaction (R8). Ozone is catalytically destroyed only if BrO recycle to Br atoms without production of ozone. This occurs through cycles e.g. the self-reaction of BrO (Reactions R9 and R10). HOBr is reformed via the reaction of BrO with HO_2, (Reaction R11), whereupon it may react again with halogen-containing aerosol to further propagate the cycle, each time doubling the concentration of reactive bromine.

Reactive uptake of HOBr consumes $H^+_{(aq)}$, thus acidity is required for prolonged BrO formation chemistry to occur. Moreover, under alkaline conditions, dissolved HOBr largely dissociates to form less reactive $BrO^-_{(aq)}$, Reaction (R12): the pKa of HOBr being 8.59 (Nagy and Ashby, 2007).

$$HOBr_{(aq)} \leftrightarrow BrO^-_{(aq)} + H^+_{(aq)} \quad \text{(R12)}$$

Alongside reactive uptake of HOBr, uptake of $BrONO_2$ (a product of the reaction of BrO and NO_2, Reaction R13) onto aerosol can also act to promote reactive bromine formation, whereupon hydrolysis generates HOBr and HNO_3 (Reactions R14 and R15). Once formed, HOBr may then react immediately with aqueous-phase halogens to produce dihalogens or may be released from the aerosol phase as HOBr (whereafter it might still undergo heterogeneous chemistry or undergo photolysis). Experimental studies indicate evidence for both HOBr and dihalogens as products from the heterogeneous reaction of $BrONO_2$. Here, the focus is on quantifying HOBr reaction kinetics as a major driver of reactive bromine formation.

$$BrO_{(g)} + NO_{2\,(g)} \rightarrow BrONO_{2\,(g)} \quad \text{(R13)}$$

$$BrONO_{2\,(g)} \rightarrow BrONO_{2\,(aq)} \quad \text{(R14)}$$

$$BrONO_{2\,(aq)} + H_2O_{(l)} \rightarrow HOBr_{(aq)} + HNO_{3\,(aq)} \quad \text{(R15)}$$

2.2 Quantifying the reactive uptake of HOBr

The reactive uptake of $\mathrm{HOBr_{(g)}}$ can be quantified by Eq. (1) (with further modification required for large particles due to the limitation of gas-phase diffusion) in terms of the reactive uptake coefficient, γ_{HOBr}, where v_{HOBr}, is the mean molecular velocity of $\mathrm{HOBr_{(g)}}$, $\mathrm{cm\,s^{-1}}$, and area, is the surface area density of the aqueous phase, $\mathrm{cm^2\,cm^{-3}}$.

γ_{HOBr} is a fractional number that quantifies the likelihood of reaction given a collision of $\mathrm{HOBr_{(g)}}$ with a particle, and can be calculated following the resistor-model framework (Eq. 2) that describes the accommodation to the aerosol, and the reaction and diffusion in or across the aerosol particle. γ_{HOBr} is a function of several parameters, including accommodation coefficient, α_{HOBr}, the solubility of HOBr, H^*, the aqueous-phase diffusion rate, D_l, the gas constant R, Temperature, T, the mean molecular velocity, v_{HOBr}, and the first-order rate constant for the reaction of $\mathrm{HOBr_{(aq)}}$, k^{I}. The parameter l is a function of D_l and k^{I}, $l = (D_l/k^{\mathrm{I}})^{0.5}$.

$$-\frac{\mathrm{d[HOBr_{(g)}]}}{\mathrm{d}t} = \gamma_{\mathrm{HOBr}} \cdot \frac{v_{\mathrm{HOBr}}}{4} \cdot [\mathrm{HOBr_{(g)}}] \cdot \mathrm{area} \tag{1}$$

$$\frac{1}{\gamma_{\mathrm{HOBr}}} = \frac{1}{\alpha_{\mathrm{HOBr}}} + \frac{v_{\mathrm{HOBr}}}{4 \cdot H^*_{\mathrm{HOBr}} \cdot R \cdot T \cdot \sqrt{D_{l,\mathrm{HOBr}} \cdot k^{\mathrm{I}}}} \cdot \frac{1}{\coth\left[\frac{r}{l}\right] - \frac{l}{r}} \tag{2}$$

$$-\frac{\mathrm{d[HOBr_{(aq)}]}}{\mathrm{d}t} = k^{\mathrm{I}} \cdot [\mathrm{HOBr_{(aq)}}] \tag{3}$$

$$k^{\mathrm{I}} = k_{\mathrm{ter}} \cdot \left[\mathrm{X^-_{(aq)}}\right] \cdot \left[\mathrm{H^+_{(aq)}}\right] \tag{4}$$

$$k^{\mathrm{I}} = k^{\mathrm{II}} \cdot \left[\mathrm{X^-_{(aq)}}\right] \tag{5}$$

To date, numerical models have adopted two approaches to simulate the reactive uptake of HOBr. Detailed process models (e.g. MISTRA; von Glasow et al. (2002), MECCA; Sander et al., 2011) tend to model HOBr gas-aerosol partitioning to and from the aerosol directly, with the reaction of HOBr inside the aerosol simulated using Eq. (3) and termolecular kinetics (Eq. 4). On the other hand, global models (e.g. in studies by von Glasow et al., 2004; Yang et al., 2005; Breider et al., 2010; Parella et al., 2012) tend to simulate HOBr reactive uptake as one step, Eq. (1), quantified by the uptake coefficient, γ_{HOBr}. The IUPAC evaluation recommends uptake coefficient to be calculated using Eq. (2) and the termolecular approach to HOBr kinetics, Eq. (4). In global models, a fixed uptake coefficient, γ_{HOBr}, is typically used for computational reasons.

However, as we highlight in this study, the termolecular kinetics approach (Eq. 4) is only valid within a limited pH range. Here we instead evaluate the reaction kinetics of $\mathrm{HOBr_{(aq)}}$ in terms of a second-order rate constant, Eq. (5), where k^{II} is a variable function of pH according to the general acid assisted reaction mechanism for $\mathrm{HOX + Y^-}$ (Sect. 4.1). Despite being well-documented (Eigen and Kustin, 1962; Kumar and Margarem, 1987; Nagy et al., 1988; Gerritsen and Margarem, 1990; Wang and Margarem, 1994) this mechanism has not been implemented in any numerical model studies of reactive halogen chemistry to date. Based on this approach we re-evaluate the reactive uptake coefficients for HOBr with k^{I} defined using Eq. (5) in terms of k^{II} instead of k_{ter}, with a parameterisation for k^{II} developed in the context of the general acid assisted mechansim. We compare our new approach to reported estimates of HOBr reactive uptake coefficients from laboratory experiments as outlined below.

2.3 Reported experimental studies on the reactive uptake of HOBr onto liquid aerosol

A number of laboratory experiments (Table 1) have quantified the reactive uptake of HOBr onto acidified sea-salt aerosol under tropospheric conditions (as well as on solid particles, not considered here).

The accommodation coefficient for HOBr onto super-saturated $\mathrm{NaBr_{(aq)}}$ aerosol was determined by Wachsmuth et al. (2002) to be $\alpha_{\mathrm{HOBr}} = 0.6 \pm 0.2$ at 298 K.

Experiments using acidified sea-salt particles made by nebulizing a 5 M NaCl and 0.5 M HCl solution under conditions representative of the troposphere found the reactive uptake coefficient for the reaction ($HOBr + Cl^-$) to be very high ($\gamma_{HOBr} > 0.2$) on deliquesced aerosol (RH > 75 %, T = 298 K), (Abbatt and Waschewsky, 1998). Conversely, experiments by Pratte and Rossi (2006) on H_2SO_4-acidified sea-salt aerosol with H_2SO_4 : NaCl molar ratio = 1.45 : 1 at 296 K measured a substantially lower HOBr uptake coefficient, $\gamma_{HOBr} \sim 10^{-2}$, with a dependence on relative humidity ($\gamma_{HOBr} \sim 10^{-3}$ below 70 % RH). This large (10^1–10^2) discrepancy has not been resolved to date. Uptake of HOBr on pure sulfate aerosol at 296 K is found to be low ($\gamma_{HOBr} \sim 10^{-3}$, Pratte and Rossi, 2006).

Aqueous-phase rate constants for the reaction of $HOBr + X^- + H^+$ have also been reported: for $HOBr + Br^-_{(aq)}$, Eigen and Kustin (1952) and Beckwith et al. (1996) report termolecular rate constants of $k_{ter} = 1.6 \times 10^{10}\ M^{-2}\ s^{-2}$ over a pH range of 2.7–3.6 and 1.9–2.4 at 298 K, respectively. For $HOBr + Cl^-_{(aq)}$, Liu and Margarem (2001) report a three-body rate constant of $2.3 \times 10^{10}\ M^{-2}\ s^{-2}$ in buffered aerosol at pH = 6.4 and 298 K. Pratte and Rossi (2006) derived first-order rate constants for the reaction of $HOBr_{(aq)}$ from their uptake experiments, finding $k^I \sim 10^3\ s^{-1}$.

The IUPAC subcommittee for gas kinetic data evaluation currently recommends an uptake coefficient parameterisation utilising accommodation coefficient $\alpha_{HOBr} = 0.6$ (Wachsmuth et al., 2002), and first-order rate constant $k^I = k_{ter} \cdot [H^+_{(aq)}] \cdot [X^-_{(aq)}]$, with $k_{ter} = 2.3 \times 10^{10}\ M^{-2}\ s^{-1}$ (Liu and Margarem, 2001) for $HOBr + Cl^-$ and $k_{ter} = 1.6 \times 10^{10}\ M^{-2}\ s^{-1}$ (Beckwith et al., 1996) for $HOBr + Br^-$. Assuming a $Cl^-_{(aq)}$ concentration of 5.3 M typical of sea-water and low uptake coefficients in alkaline sea-salt aerosol (IUPAC evaluation, see website, e.g. Ammann et al., 2013), this parameterisation yields a high uptake coefficient, $\gamma_{HOBr} \sim 0.6$, on acidified sea-salt aerosol, and is in agreement with $\gamma_{HOBr} \geq 0.2$ reported by Abbatt and Waschewsky (1998) while overestimating the uptake coefficient as reported by Pratte and Rossi (2006) by a factor of ~ 20.

Here we present new uptake calculations based on the general acid assisted mechanism rather than termolecular kinetics in an attempt to consolidate these contrasting reported uptake coefficients within a single framework for the first time, and explain differences between model predictions and field observations of reactive bromine in the marine environment, as well as making first predictions of HOBr reactive uptake coefficients in volcanic plumes.

3 Method

3.1 A new parameterisation for the rate constant for HOBr + $X^-_{(aq)}$

Critical to this re-evaluation of γ_{HOBr} is the parameterisation of the rate of reaction of HOBr with Br^- or Cl^- in terms of a second-order rate constant, k^{II}, that is a function of particle acidity, in line with the general acid assisted mechanism (Eigen and Kustin, 1962). The first-order rate constant, k^{I} can then be determined as the product of the second-order rate constant, k^{II}, and the concentration of halide ion $X^-_{(aq)}$; $k^{\mathrm{I}} = k^{\mathrm{II}} \cdot [X^-_{(aq)}]$. This contrasts to previous approaches that assumed termolecular kinetics with $k^{\mathrm{I}} = k_{\mathrm{ter}} \cdot [X^-_{(aq)}] \cdot [H^+_{(aq)}]$.

Parameterisations for k^{II} were derived as a function of acidity using kinetic theory of the general acid assisted mechanism, and available laboratory data. To determine the aerosol composition, specifically halide concentration, $[X^-_{(aq)}]$, and acidity, we use the E-AIM (Extended-Aersol Inorganic) model and Henry's constants (see below). Given high ionic strength of the solutions studied, concentrations were converted to activities using activity coefficients provided by E-AIM.

3.2 Definition of other parameters in the uptake equation, for sulphuric acid and sea-salt aerosol

Further parameters to calculate the uptake coefficient for HOBr (Eq. 2) were defined as follows. The accommodation coefficient, α_{HOBr} was set to 0.6, following experimental findings by Wachsmuth et al. (2002) who measured accommodation-limited uptake onto $\mathrm{NaBr_{(aq)}}$ particles under very low $\mathrm{HOBr_{(g)}}$ concentrations. It is assumed that this accommodation coefficient is also representative for acidified $\mathrm{NaCl_{(aq)}}$ or $\mathrm{H_2SO_{4\,(aq)}}$ particles in the troposphere. Temperature, $T = 298\,\mathrm{K}$ unless otherwise stated, the ideal gas constant $R = 8.206\times10^{-2}\,\mathrm{L\,atm\,K^{-1}\,mol^{-1}}$. The particle radius, r, was set to $r = 1$ or $r = 0.1\,\mu\mathrm{m}$, noting the occurrence of both supra- and submicron aerosol in the marine environment and volcanic plumes. The diffuso-reactive length-scale, l, describes the typical distance over which reaction occurs, with $l = (D_{l,\mathrm{HOBr}}/k^{\mathrm{I}})^{0.5}$.

This study focuses primarily on HOBr reactive uptake under acidic aerosol conditions. In order to account for the dissociation of HOBr under alkaline conditions, we used a modified HOBr rate constant to reflect the dissociation of $\mathrm{HOBr_{(aq)}}$ into $\mathrm{BrO^-}$ at high pH. We also assumed $\mathrm{BrO^-_{(aq)}}$ is unreactive to $\mathrm{X^-_{(aq)}}$. Thus, $k^{\mathrm{II}} = k^{\mathrm{II}}\cdot[\mathrm{Cl^-_{(aq)}}]\cdot[\mathrm{H^+_{(aq)}}]/([\mathrm{H^+_{(aq)}}]+K_\mathrm{a})$, where the acid dissociation constant is $K_\mathrm{a} = 2.6\times10^{-9}\,\mathrm{mol\,L^{-1}}$ (given a pKa for HOBr of 8.59, Swain, 1983; Nagy and Ashby, 2007), and where the term $[\mathrm{H^+_{(aq)}}]/([\mathrm{H^+_{(aq)}}]+K_\mathrm{a})$ reflects the fraction of dissolved $\mathrm{HOBr_{(aq)}}$ in that remains in the form HOBr.

Two parameterisations for the aqueous-phase diffusion constant for HOBr, D_l, $\mathrm{m^2\,s^{-1}}$, and the solubility of HOBr, H^*, $\mathrm{mol\,L^{-1}\,atm^{-1}}$, for salt solutions and sulphuric acid solutions are used. The former applies for weakly acidified sea-salt aerosol (and is the approach used in studies to date), whereas we consider the latter more appropriate for highly $\mathrm{H_2SO_4}$-acidified sea-salt aerosol and volcanic aerosol.

We use $D_{l,\mathrm{HOBr}} = 1.42\times10^{-5}\,\mathrm{m^2\,s^{-1}}$ reported by Frenzel et al. (1998) for HOBr diffusion in salt solutions at 291 K, which we apply directly in this study at 298 K. For HOBr diffusion in sulphuric acid solutions, the parameterisation Eq. (6) is used following Klassen et al. (1998), where T is the temperature in K, and η is the viscosity of sulfuric acid that given by Eq. (7). $c_{\mathrm{HOBr}} = 6.2\times10^8$ for HOBr, $B = 425$, $n = -1.43$, A and T_0 are functions of the wt%H_2SO_4, (wt): $A = 279.4-8.8\cdot\mathrm{wt}+0.358\cdot\mathrm{wt}^2$, $T_0 = 203-2.6\cdot\mathrm{wt}+0.0287\cdot\mathrm{wt}^2$, where the wt%$H_2SO_4$ was determined using the E-AIM thermodynamic model. This parameterisation is valid for 30 wt % to 72 wt % sulfuric acid at temperatures between 220 and 300 K. D_l at lower wt% sulphuric acid (high RH) was estimated by interpolation across the RH and Temperature parameter space, and extrapolation to high RH, yielding a diffusion rate comparable to that of water at very high humidity, i.e. $1.42\times10^{-5}\,\mathrm{m^2\,s^{-1}}$.

$$D_{l,\mathrm{HOBr}} = \frac{c_{\mathrm{HOBr}}\cdot T}{\eta} \tag{6}$$

$$\eta = A\cdot T^{n}\cdot \exp[B/(T-T_0)] \tag{7}$$

HOBr solubility in weakly acidified sea-salt aerosol is represented using the value for water, $6.1\times10^3\,\mathrm{M\,atm^{-1}}$ at 291 K, (Frenzel et al., 1998), which we apply directly to this study at 298 K, consistent with the value of $> 1.9\times10^3\,\mathrm{mol\,L^{-1}\,atm^{-1}}$ at 298 K estimated by Blatchley et al., (1991). For HOBr solubility in $H_2SO_{4\,(aq)}$ we use a parameterisation derived by Iraci et al. (2005) based on measurements over 201–252 K in 45–70 wt% H_2SO_4. In application of this parameterisation, Eq. (8), to the troposphere, we note that the wt%H_2SO_4 only exceeds 45 % in the troposphere if relative humidity is less than ~ 40–50 %. However, Iraci et al. (2005) report that the dependence of solubility, H*, on acid concentration is relatively weak. The parameterisation yields an RH-independent HOBr solubility in sulphuric acid of $4\times10^2\,\mathrm{M\,atm^{-1}}$ at 298 K (i.e. an order of magnitude lower than that assumed for water at this temperature), rising to $10^3\,\mathrm{M\,atm^{-1}}$ at 273 K and $10^4\,\mathrm{M\,atm^{-1}}$ at 253 K.

$$\log_{10}\left(H^{*}_{\mathrm{HOBr-H_2SO_{4\,(aq)}}}\right) = \frac{2349}{T} - 5.27 \tag{8}$$

3.3 Aerosol composition estimated using the E-AIM thermodynamic model

The E-AIM (Extended Aerosol Inorganic Model) thermodynamic model was used to predict the composition of both acidified sea-salt and volcanic aerosol and in particular the halide concentration, X^-_{aq}. We used E-AIM version I that considers the H^+–SO_4^{2-}–NO_3^-–Cl^-–Br^-–H_2O system between 200 to 330 K (Carslaw et al., 1995), and model version III that considers the H^+–NH_4^+–Na^+–SO_4^{2-}–NO_3^-–Cl^-–H_2O system at 298 K (Clegg et al., 1998).

Inputs to E-AIM include the temperature, relative humidity and total SO_4^{2-}, Cl^-, Br^-, Na^+, and H^+ in the system defined in $mol\,m^{-3}$ volume of atmosphere. Outputs include the number of moles per m^3 of atmosphere of $Na^+_{(aq)}$, $SO^{2-}_{4\,(aq)}$, $HSO^-_{3\,(aq)}$, $H^+_{(aq)}$, $Br^-_{(aq)}$, $Cl^-_{(aq)}$, $HCl_{(g)}$, $HBr_{(g)}$, the activity coefficients for these species, and the total aerosol volume ($cm^3\,m^{-3}$). It was thereby possible to calculate the aqueous-phase concentrations and activities of halides and $H^+_{(aq)}$ in the aerosol, in $mol\,L^{-1}$.

Because E-AIM model versions cannot predict the composition of aerosol which contains all four components: Na^+, SO_4^{2-}, Br^- and Cl^-, calculations for sea-salt aerosol were performed with E-AIM version III (see composition above), with bromide concentration calculated subsequently. For simplicity we ignore other possible sea-salt ions (e.g. Mg^{2+}, Ca^{2+}, NH_4^+, NO_3^-) therefore our assumed Na : Cl ratio (1 : 1) is slightly higher than that of actual sea-water (0.4685 : 0.5459 = 0.86 : 1), Wilson (1975). The aerosol $Br^-_{(aq)}$concentration was then predicted as follows: total Br concentration was calculated assuming a Br : Na molar ratio corresponding to that of sea-water (0.000842 : 0.4685 = 0.0018), Wilson (1975). The relative concentrations of $HBr_{(g)}$ and $Br^-_{(aq)}$ were described using the effective Henry's solubility for HBr, H^* (Eq. 9). H^* is a function of the acid dissociation constant ($K_a = 10^9$ M, Schweitzer et al., 2000), and $H^+_{(aq)}$ concentration (determined from the E-AIM model output, noting that HBr contributes negligibly to aerosol acidity compared to H_2SO_4). For a closed system, the partitioning between $HBr_{(g)}$ and $Br^-_{(aq)}$ also depends on the total aerosol volume, and was calculated using Eq. (10) (Seinfeld and Pandis, 2006), involving the HBr solubility, H^* (mol L^{-1} atm^{-1}) the total bromine concentration Br in the system (in moles per L of air), the gas constant, R defined earlier), Temperature T in Kelvin, and the liquid water content, $w_L = L \times 10^{-6}$, where L is the total aerosol volume density (g m^{-3}) determined from the E-AIM output (for a specified sea-salt concentration in moles m^{-3} and degree of acidification). E-AIM model simulations were performed for aerosol under reported laboratory conditions of experiments quantifying the HOBr uptake coefficient (see Sects. 4.4.2 and 4.4.3), and for a "simple" model sea-salt aerosol to demonstrate the effect of progressive H_2SO_4-acidification (Sects. 4.4.1 and 5.1). This "simple" model sea-salt aerosol composition does not include carbonate buffering (or the effect of other potential impurities such as ammonium). The model aerosol composition is independent of the particle radius, r (which nevertheless affects the uptake coefficient calculated according to Eq. 2).

$$H^*_{\mathrm{HBr}} = \frac{1.3 \cdot 10^9}{K_a} \cdot \left(1 + K_a / \left[\mathrm{H}^+_{(\mathrm{aq})}\right]\right) \tag{9}$$

$$\left[\mathrm{Br}^-_{(\mathrm{aq})}\right] = H^*_{\mathrm{HBr}} \cdot \frac{[\mathrm{Br}_t] \cdot R \cdot T}{1 + H^*_{\mathrm{HBr}} \cdot w_L \cdot R \cdot T} \tag{10}$$

E-AIM model version I was used to predict volcanic aerosol composition, particularly concentrations of both $\mathrm{Br}^-_{(\mathrm{aq})}$ and $\mathrm{Cl}^-_{(\mathrm{aq})}$, over a range of tropospheric RH (0.4–0.99) and temperature (300–230 K). We assumed a volcanic composition of $(\mathrm{SO_2}) : \mathrm{Cl}^- : \mathrm{Br}^- : \mathrm{SO}_4^{2-}$ of 1 : 0.5 : 0.00075 : 0.01 that is typical for an Arc (subduction zone) volcano such as Etna (note SO_2 simply listed as a reference volcanic gas but is not included in the E-AIM calculation). We also consider an evolved-plume situation where significant BrO chemistry has taken place, causing $[\mathrm{Br}^-_{(\mathrm{aq})}]$ to become depleted to $\mathrm{Br}^- : \mathrm{Cl}^- = 7 \times 10^{-5}$ (according to the equilibria of Wang et al., 1994). Anions were balanced by H^+ as the cation. The $\mathrm{SO}_4^{2-} : \mathrm{SO_2}$ ratio assumed here is based on crater-rim measurements that indicate sulphate : SO_2 molar ratio of ∼ 1 : 100 (e.g. Mather et al., 2003). This "quasi-direct" volcanic emission of sulfate is believed to be caused by high-temperature production of SO_3 in the near-vent plume (Mather et al., 2003) followed by lower temperature reaction with H_2O (Roberts et al., 2009). For the abovementioned volcanic emission composition, the absolute concentrations required for the E-AIM input (in $\mathrm{mol\,m^{-3}}$) were calculated for three different plume strengths equivalent to an SO_2 gas concentration of 30, 3, and 0.3 $\mathrm{\mu mol\,m^{-3}}$ which is equivalent to approximately 1, 0.1 and 0.01 ppmv SO_2 at 4 km altitude (US standard atmosphere).

4 Results

In this section we present our parameterisation of the second order rate coefficient as a function of aerosol acidity, using both existing experimental data and the E-AIM.

4.1 The kinetics of HOBr+X⁻ according to the general acid assisted mechanism

The HOBr reaction with X^- in acidic aerosols has been described using the general-acid assisted mechanism (Eigen and Kustin, 1962), summarized below (Reactions R16–R20), in which an equilibrium is established between $HOBrX^-_{(aq)}$ and HOBr according to the rate constants of Reactions (R16) and (R17), k_1 and k_{-1}. The formation of products, Reaction (R18), involves a transition-state, $[H_2OBrX_{(aq)}]^{TS}$ that is stabilised by proton-donation to the oxygen, with overall rate constant k_H. Moreover, formation of products can also occur at low acid concentrations via a slower pathway, Reaction (R19), followed by fast Reaction (R20), with overall rate constant k_0. We first derive an expression for k^{II} according to combined mechanism, in terms of the underlying rate constants k_1, k_{-1}, k_0 and k_H, which we will then apply to an analysis of reported reactive uptake coefficients.

$$HOBr_{(aq)} + X^-_{(aq)} \xrightarrow{k_1} HOBrX^-_{(aq)} \quad \text{(R16)}$$

$$\mathrm{HOBrX^-_{(aq)}} \xrightarrow{k_{-1}} \mathrm{HOBr_{(aq)}} + \mathrm{X^-_{(aq)}} \tag{R17}$$

$$\mathrm{HOBrX^-_{(aq)}} + \mathrm{H^+_{(aq)}} \xrightarrow{k_\mathrm{H},\ [\mathrm{H_2OBrX_{(aq)}}]^\mathrm{TS}} \mathrm{H_2O_{(aq)}} + \mathrm{BrX_{(aq)}} \tag{R18}$$

$$\mathrm{HOBrX^-_{(aq)}} \xrightarrow{k_0} \mathrm{OH^-_{(aq)}} + \mathrm{BrX_{(aq)}} \tag{R19}$$

$$\mathrm{OH^-_{(aq)}} + \mathrm{H^+_{(aq)}} \xrightarrow{\text{fast}} \mathrm{H_2O_{(aq)}} \tag{R20}$$

The combination of Reactions (R16)–(R19) leads to Eq. (11). Assuming $[\mathrm{HOBrX^-_{(aq)}}]$ is in equilibrium leads to Eq. (12).

$$\frac{\mathrm{d}\left[\mathrm{HOBrX^-_{(aq)}}\right]}{\mathrm{d}t} = k_1 \cdot [\mathrm{HOBr_{(aq)}}] \cdot \left[\mathrm{X^-_{(aq)}}\right] - k_{-1} \cdot \left[\mathrm{HOBrX^-_{(aq)}}\right] - k_\mathrm{H} \cdot \left[\mathrm{HOBrX^-_{(aq)}}\right] \cdot \left[\mathrm{H^+_{(aq)}}\right] - k_0 \cdot \left[\mathrm{HOBrX^-_{(aq)}}\right] = 0 \tag{11}$$

$$\left[\mathrm{HOBrX^-_{(aq)}}\right] = \frac{k_1 \cdot [\mathrm{HOBr_{(aq)}}] \cdot \left[\mathrm{X^-_{(aq)}}\right]}{k_{-1} + k_0 + k_\mathrm{H} \cdot \left[\mathrm{H^+_{(aq)}}\right]} \tag{12}$$

The rate of reaction of $\mathrm{HOBr_{(aq)}}$ is equal to the rate of production of $\mathrm{BrX_{(aq)}}$, given by Eq. (13). Substitution of the equation for $[\mathrm{HOBrX^-_{(aq)}}]$, Eq. (12), into the rate equation Eq. (13), yields Eq. (14), enabling the second-order rate constant, k^II, to be defined in terms of k_1, k_0, k_H and $[\mathrm{H^+_{(aq)}}]$, Eq. (15).

$$-\frac{\mathrm{d}[\mathrm{HOBr_{(aq)}}]}{\mathrm{d}t} = \frac{\mathrm{d}[\mathrm{BrX_{(aq)}}]}{\mathrm{d}t} = k_\mathrm{H} \cdot \left[\mathrm{HOBrX^-_{(aq)}}\right] \cdot \left[\mathrm{H^+_{(aq)}}\right] + k_0 \cdot \left[\mathrm{HOBrX^-_{(aq)}}\right] \tag{13}$$

$$\frac{\mathrm{d}[\mathrm{BrX_{(aq)}}]}{\mathrm{d}t} = \left(k_\mathrm{H} \cdot \left[\mathrm{H^+_{(aq)}}\right] + k_0\right) \cdot \frac{k_1 \cdot [\mathrm{HOBr_{(aq)}}] \cdot \left[\mathrm{X^-_{(aq)}}\right]}{k_{-1} + k_0 + k_\mathrm{H} \cdot \left[\mathrm{H^+_{(aq)}}\right]} = \frac{k_1 \cdot \left(k_\mathrm{H} \cdot \left[\mathrm{H^+_{(aq)}}\right] + k_0\right)}{k_{-1} + k_0 + k_\mathrm{H} \cdot \left[\mathrm{H^+_{(aq)}}\right]}$$

$$\cdot [\mathrm{HOBr}_{(\mathrm{aq})}] \cdot \left[\mathrm{X}^{-}_{(\mathrm{aq})}\right] \tag{14}$$

$$k^{\mathrm{II}} = \frac{k_1 \cdot \left(k_0 + k_{\mathrm{H}} \cdot \left[\mathrm{H}^{+}_{(\mathrm{aq})}\right]\right)}{k_{-1} + k_0 + k_{\mathrm{H}} \cdot \left[\mathrm{H}^{+}_{(\mathrm{aq})}\right]} \tag{15}$$

Simplifications to Eq. (15) can be made in the limits of high and low acidity (Eqs. 16 and 17), finding k^{II} is independent of aerosol acidity in both cases. For a mid-range acidity ($k_{\mathrm{H}} \cdot [\mathrm{H}^{+}_{(\mathrm{aq})}] \ll k_{-1} + k_0$), we can show by rewriting Eq. (15) to yield Eq. (18) that k^{II} becomes linearly dependent on the acidity. In this mid-acidity regime (only), the acid-dependence is equal to the three-body or termoleuclar rate constant, $k_1 \cdot k_{\mathrm{H}} / (k_{-1} + k_0) = k_{\mathrm{ter}}$.

$$k^{\mathrm{II}} = k_1 \text{ at high acidity (the limit as } \mathrm{H}^{+}_{(\mathrm{aq})} \text{ tends to infinity)} \tag{16}$$

$$k^{\mathrm{II}} = \frac{k_1 \cdot k_0}{k_{-1} + k_0} \text{ at very low acidity (the limit as } \mathrm{H}^{+}_{(\mathrm{aq})} \text{ tends to zero)} \tag{17}$$

$$k^{\mathrm{II}} = \frac{k_1 \cdot k_0}{k_{-1} + k_0} + \frac{k_1 \cdot k_{\mathrm{H}} \cdot \left[\mathrm{H}^{+}_{(\mathrm{aq})}\right]}{k_{-1} + k_0} \tag{18}$$

Equations (15)–(18) describe k^{II} in terms of four underlying rate constants (k_1, k_{-1}, k_0, k_{H}) and the aerosol acidity. However, quantifying these underlying rate constants using published data is somewhat challenging given the limited experimental data. This is now attempted below.

4.2 Estimating the underlying rate constants (k_1, k_{-1}, k_0, k_{H}) for HOBr + Br$^-$ and HOBr + Cl$^-$

A number of aqueous-phase rate constants for the reaction of HOBr + X$^-$ + H$^+$ have been reported: for HOBr + Br$^-_{(\mathrm{aq})}$, Eigen and Kustin (1952) and Beckwith et al. (1996) report termolecular rate constants of $k_{\mathrm{ter}} = 1.6 \times 10^{10}\,\mathrm{M^{-2}\,s^{-2}}$ over a pH range of 2.7–3.6 and 1.9–2.4 at 298 K, respectively. These experiments quantified the rate of reaction in the termolecular regime only, although Eigen and Kustin (1962) used a consideration of relative stability constants across the halogen series: HOCl + Cl, HOBr + Br and HOI + I to attempt to estimate underlying rate constants.

Using the reported experimental data, k^{II} parameterisations (in terms of the underlying rate constants (k_1, k_{-1}, k_0 and k_{H}) and acidity according to Eq. (15) derived above) are estimated as follows.

For HOBr + $\mathrm{Br^-}$, the underlying rate constants are based on Eigen and Kustin (1962), who proposed order of magnitude estimates of $k_1 = 5 \times 10^9\,\mathrm{M^{-1}\,s^{-1}}$, $k_{-1} = 5 \times 10^9\,\mathrm{s^{-1}}$, $k_{\mathrm{H}} = 2 \times 10^{10}\,\mathrm{M^{-1}\,s^{-1}}$, and $k_0 = 10^4\,\mathrm{s^{-1}}$. The following modification is made, on the basis of data from Beckwith et al. (1996). In Fig. 4 of Beckwith et al. (1996), we observe indications of acid-saturation in their k^{II} rate constant data for HOBr + $\mathrm{Br^-}$, seen as curvature in the plots of observed k^{II} vs. acidity. This is also seen in their Fig. 5 where $k^{\mathrm{II}}_{\mathrm{observed}} \geq 2.3 \times 10^8\,\mathrm{M^{-1}\,s^{-1}}$. We therefore suggest acid-saturation may occur around an order of magnitude lower than Eigen and Kustin's estimate of $k^{\mathrm{II}} \sim 5 \times 10^9\,\mathrm{M^{-1}\,s^{-1}}$ for HOBr + $\mathrm{Br^-_{(aq)}}$, i.e. potentially $k^{\mathrm{II}} \sim 5 \times 10^8\,\mathrm{M^{-1}\,s^{-1}}$. We therefore estimate $k_1 \sim 5 \times 10^8\,\mathrm{M^{-1}\,s^{-1}}$ (Eq. 16) and also adjust k_{-1} to $k_{-1} \sim 5 \times 10^8\,\mathrm{s^{-1}}$ noting the reported stability constant $k_1/k_{-1} \sim 1\,\mathrm{M^{-1}}$, according to Eigen and Kustin (1962). However, any evidence for acid-saturation lays within the reported error bars for the data points. In any case the abovementioned adjustment does not affect the general conclusions about $\gamma_{\mathrm{HOBr+Br}}$ in this study.

For HOBr + $\mathrm{Cl^-_{(aq)}}$, Liu and Margarem (2001) report a three-body rate constant of $2.3 \times 10^{10}\,\mathrm{M^{-2}\,s^{-2}}$ in buffered aerosol at pH = 6.4 and 298 K. Pratte and Rossi (2006) also report estimates for first-order rate constants for reaction of $\mathrm{HOBr_{(aq)}}$ derived from their uptake coefficient experiments. Their reported experimental data is re-interpretted below to contribute further quantification to the reaction kinetics of HOBr + $\mathrm{Cl^-}$.

For HOBr + Cl^-, the underlying rate constants (k_1, k_{-1}, k_H, k_0) are estimated as follows. The rate constant k_1 is derived from the estimation of k^{II} at acid saturation (Eq. 16). For this, we estimated k^{II} at pH −1 to 0 from experiments of Pratte and Rossi (2006), Table 2. The new k^{II} estimates are derived from first order k^{I} rate constants for the reaction of $HOBr_{(aq)}$, reported by Pratte and Rossi (2006), based on their uptake experiments on H_2SO_4-acidified sea-salt aerosol at H_2SO_4 : NaCl of 1.45 : 1, 296 K and RH = 0.77–0.9. Our derivation of k^{II} from the reported k^{I} requires aerosol chloride concentration to be known, as $k^{II} = k^{I}/[Cl^-_{(aq)}]$. We utilise the estimates of $[Cl^-_{(aq)}]$ under the experimental conditions as predicted by the E-AIM model, that predicts chloride concentrations are reduced under the experimental conditions as consequence of acid-displacement of $HCl_{(g)}$ (see further discussion in Sect. 4.4). Our evaluation of rate constants from the experimental data reported by Pratte and Rossi (2006) yields $k^{II} \sim 10^4\,M^{-1}\,s^{-1}$ over pH −1 to 0, see Table 2 for details. We note that in their reporting of k^{I} rate constants from their uptake experiments, Pratte and Rossi, (2006) assumed an accommodation coefficient of either $\alpha_{HOBr} = 0.2$ or $\alpha_{HOBr} = 0.02$. Given that experiments on $NaBr_{(aq)}$ aerosol have identified an accommodation coefficient for HOBr on $NaBr_{(aq)}$ particles of 0.6 (Wachsmuth et al., 2002), the k^{II} data derived assuming $\alpha_{HOBr} = 0.2$ are likely more representative. Nevertheless, either case yields estimate for $k^{II} \sim 10^4\,M\,s^{-1}$ over pH = 0 to −1. A further estimate for k^{II} is derived from the reported three-body rate constant of $2.3 \times 10^{10}\,M^{-2}\,s^{-2}$ at pH = 6.4, by setting $k^{II} = k_{ter} \cdot [H^+_{(aq)}]$. This yields $k^{II} = 9 \times 10^3\,M^{-1}\,s^{-1}$ at pH 6.4.

Thus, collectively these two datasets at pH = 6.4 and 0 to −1 suggest that k^{II} is acid saturated at $\sim 10^4\,M\,s^{-1}$ at pH ≤ 6. Based on this value for k^{II} at acid saturation (where $k^{II} = k_1$) we set $k_1 = 1.2 \times 10^4\,M\,s^{-1}$, as an average estimate. This k_1 estimate for HOBr + Cl^- is less than k_1 for HOBr + Br^-, consistent with the greater nucleophile strength of Br^- compared to Cl^-. A number of choices for k_0, k_{-1} and k_H might be made, but we choose to fix $k_H = 2 \times 10^{10}\,M^{-1}\,s^{-1}$ to be equal to that estimated by Eigen and Kustin (1961) for HOBr + Br^- noting this reaction likely close to the diffusion limit.

We expect that k^{II} for HOBr + Cl$^-$ at low acidity (= $(k_1 \cdot k_0)/(k_0 + k_{-1})$) is of similar order of magnitude to the k^{II} estimate for HOCl + Cl$^-$ ($\leq 0.16\,\mathrm{M^{-1}\,s^{-1}}$, see Gerritsen and Margarem, 1989) or perhaps slightly higher (because the less electronegative Br of HOBr may be more susceptible to nucleophilic attach than HOCl), but substantially less than the k^{II} estimate for HOBr + Br$^-$ ($10^4\,\mathrm{M^{-1}\,s^{-1}}$, Eigen and Kustin, 1962) at low acidity, given Cl$^-$ is a weaker nucleophile than Br$^-$. Here, we set the low acidity k^{II} rate constant; $(k_0 \cdot k_1)/(k_1 + k_{-1}) = 10^1\,\mathrm{M^{-1}\,s^{-1}}$. A further constraint is the reported three-body rate constant of $2.3 \times 10^{10}\,\mathrm{M^{-2}\,s^{-1}}$ (Liu and Magarem, 2002). This is commonly interpreted as a termolecular rate constant, k_{ter}, although the experimental data do not prove that this rate constant is in fact in the termolecular regime. Nevertheless, assuming $k_{\mathrm{ter}} = 2.3 \times 10^{10}\,\mathrm{M^{-2}\,s^{-1}} = k_{\mathrm{H}} \cdot k_1/(k_0 + k_{-1})$ and setting the low acidity k^{II} rate constant, $(k_0 \cdot k_1)/(k_1 + k_{-1}) = 10^1\,\mathrm{M^{-1}\,s^{-1}}$ as mentioned above, with $k_1 = 1.2 \times 10^4\,\mathrm{M^{-1}\,s^{-1}}$, yielding $k_0 = 2 \times 10^1\,\mathrm{M^{-1}\,s^{-1}}$ and $k_{-1} = 1.1 \times 10^4\,\mathrm{s^{-1}}$. Alternatively, setting the low acidity k^{II} rate constant to $(k_0 \cdot k_1)/(k_1 + k_{-1}) = 10^0\,\mathrm{M^{-1}\,s^{-1}}$(i.e. closer to the estimate for HOCl + $\mathrm{Cl^-_{(aq)}}$) yields $k_0 = 10^0\,\mathrm{M^{-1}\,s^{-1}}$ and $k_{-1} = 1.0 \times 10^4\,\mathrm{s^{-1}}$. These estimates for the underlying rate constants for HOBr + Cl$^-$ are rather uncertain, nevertheless the most important result is the acid-saturation of k^{II} for HOBr + Cl$^-$, which the experimental data suggests occurs at $\sim 10^4\,\mathrm{M\,s^{-1}}$ at pH ≤ 6.

4.3 A new parameterisation for the k^{II} for HOBr + Br$^-$ and HOBr + Cl$^-$

The underlying rate constants (k_1, k_{-1}, k_{H}, k_0) for reaction of HOBr+Br$^-$ and HOBr+Cl$^-$ estimated above are summarized in Table 3. Our parameterisation for k^{II} based on these data, with k^{II} defined by Eq. (15) is shown in Fig. 1 as a function of aerosol acidity, alongside the experimental values for k^{II} derived from the reported experimental data from Eigen and Kustin (1962), Beckwith et al. (1996), Liu and Margarem (2001) and Pratte and Rossi (2006) (see Table 2). As expected, the k^{II} parameterisations for HOBr + Br$^-$ and HOBr + Cl$^-$ exhibit three distinct regimes: k^{II} is independent of acidity at high pH. k^{II} is dependent on acidity for a medium pH range, where the rate constant $k^{II} = k_{ter} \cdot [H^+_{(aq)}]$, and in this regime the rate constant is termolecular. At high acidity, k^{II} becomes acid-independent ($k^{II} = k_1$), yielding an acid-saturated k^{II} that is lower for $HOBr + Cl^-$ than $HOBr + Br^-$ given the weaker nucleophile strength.

Also shown in Fig. 1 is the the termolecular approach to HOBr kinetics assumed to date, which predicts acid-dependent k^{II} over all parameter space. Clearly, the termolecular assumption for HOBr kinetics is only valid in the termolecular regime, between pH 1–6 for $HOBr + Br^-$, and > pH 6 for $HOBr + Cl^-$. At high acidity, the termolecular approach overestimates the rate constant compared to the k^{II} parameterisation by several orders of magnitude. The disagreement is greatest for $HOBr + Cl^-$, where the termolecular approach overestimates the k^{II} rate constant by a factor of 10^3 at pH = 3 and 10^6 at pH = 0 (overestimations respectively equivalent to ~ 100 thousand and ~ 100 million percent of the revised rate constant value). Of interest is the effect of our revised parameterisation on the HOBr reactive uptake coefficient. Below we use our revised k^{II} parameterisation to evaluate uptake coefficients under laboratory experimental conditions. In Sect. 5 we evaluate the HOBr reactive uptake coefficient in the marine environment and volcanic plumes and discuss implications for reactive halogen chemistry in these environments.

4.4 Comparison of our model with experimental uptake coefficient data

As discussed in the introduction, discrepancies exist in the reported reactive uptake coefficients for HOBr on acidified sea-salt aerosol. Abbatt and Waschewsky (1998) observed a strong pH dependence of the uptake onto sodium chloride aerosol, being 1.5×10^{-3} for neutral, unbuffered sodium chloride aerosol, rising to > 0.2 for aerosols acidified to pH 0.3 by the addition of HCl, i.e. close to the accommodation coefficient ($\alpha = 0.6 \pm 0.2$, Wachsmuth et al., 2002). The role of H^+ species in the reactive uptake process was further demonstrated by the high uptake coefficient of > 0.2 on aerosols buffered to pH 7 by a NaH_2PO_4/Na_2HPO_4 buffer. In contrast, Pratte and Rossi (2006) measured reactive uptake coefficients on H_2SO_4-acidified sea-salt aerosol to be ~ 10^{-2} at $H_2SO_4 : NaCl = 1.45 : 1$, with an RH-dependence (finding $\gamma_{HOBr} \sim 10^{-3}$ at RH < 70 %).

Here we show that the origin for this wide discrepancy between measured HOBr uptake onto acidified bromide aerosol and chloride aerosol lies partly in the difference in reactivity of HOBr towards Br^- and Cl^-, but also in the different aerosol composition in the two cases.

4.4.1 Composition of acidified sea-salt aerosol

The uptake experiments of Abbatt and Waschewsky (1998) and Pratte and Rossi (2006) respectively involve HCl and H_2SO_4 as acidifying agents of the sea-salt aerosol. These are known to exert contrasting impacts on the aerosol composition, as summarized below.

General results for a model sea-salt aerosol that undergoes progressive H_2SO_4 acidification are given in Fig. 2, based on a single mode sea-salt aerosol, with a PM_{10} concentration of 10 µg m^{-3} (Seinfeld and Pandis, 2006), which is equivalent to 0.1 µmol m^{-3} Na^+ at 80 % RH and 298 K according to E-AIM calculations of $NaCl_{(aq)}$. Having set [Cl] = [Na], we vary the H_2SO_4 : Na molar ratio from 0.05 to 400 and use E-AIM to determine the equilibrium aerosol composition, with bromide and HBr partitioning determined using Henry's law (see Methods).

The H_2SO_4-acidification induces acid-displacement of $HCl_{(g)}$, which occurs around $H_2SO_4 : Na \geq 0.4$ for the model aerosol., depleting $Cl^-_{(aq)}$ concentrations. Further addition of $H_2SO_{4(aq)}$ acts to increase the total aerosol volume but does not in fact dilute $[Cl^-_{(aq)}]$ given the presence of a $HCl_{(g)}$ reservoir that responds by increased $HCl_{(g)}$ to $Cl^-_{(aq)}$ partitioning. Conversely, acid-displacement of $HBr_{(g)}$ is less effective due to the higher solubility of HBr (e.g. Sander, 1999), and the increasing aerosol volume (as consequence of the additional $H_2SO_{4(aq)}$) acts to dilute $Br^-_{(aq)}$ (as well as $Na^+_{(aq)}$) at high H_2SO_4 : Na. Note that in our model aerosol HBr temporarily partitions to the gas-phase upon addition of $H_2SO_{4\,(aq)}$ but returns to the aqueous-phase at higher $H_2SO_4 : Na$ ratios as consequence of the increasing total aerosol volume. However, in a real marine environment with multiple aerosol modes, bromide might largely remain in the aqueous-phase. In any case, there exists no $HBr_{(g)}$ reservoir at high $H_2SO_4 : Na$ ratios; bromide concentrations are diluted but the bromide : sodium ratio in the aerosol still reflects that of sea-salt. In summary, halide concentrations are reduced in H_2SO_4-acidified sea-salt aerosol both by acid-displacement of $HCl_{(g)}$ and by dilution of $Br^-_{(aq)}$ by the additional $H_2SO_{4\,(aq)}$ volume upon a high degree of H_2SO_4-acidification. Similar HCl-displacement is expected to occur for HNO_3-acidification of sea-salt aerosol, but not for acidification of sea-salt aerosol by HCl.

4.4.2 High uptake coefficient on HCl-acidified sea-salt aerosol

In contrast to the H_2SO_4-acidified sea-salt aerosol case shown above, HCl-acidification of sea-salt aerosol does not induce significant acid-displacement of $HCl_{(g)}$. Here we illustrate how $Cl^-_{(aq)}$ concentrations in HCl-acidified sea-salt aerosol remain high so as to yield a high uptake coefficient

E-AIM model III calculations were performed for HCl-acidified sea-salt aerosol at HCl : NaCl = 0.1 : 1, 298 K and 80 % RH (above deliquescence), according to experimental conditions of Wachewsky and Abbatt, 1998. Whilst the experimental aerosol consisted of a bimodal distribution of both large (few µm) and small (< µm) particles, the larger particles (range 1–5 µm diameter, number density 1×10^4–$4 \times 10^4\,cm^{-3}$, surface area 1×10^3–$6 \times 10^3\,cm^2\,cm^{-3}$) were reported to dominate the observed HOBr uptake. For our calculations we assumed aerosol of 2 µm diameter and number density of $1 \times 10^4\,cm^{-3}$, which yields a surface area density of $1.2 \times 10^3\,cm^2\,cm^{-3}$ and volume density of $4.1 \times 10^{-8}\,cm^3\,cm^{-3}$. This aerosol volume density is approximately equivalent to a pure deliquesced sea-salt concentration of 0.2 µmoles m^{-3} Na at 76 % RH and 298 K according to E-AIM. Addition of 0.02 µmol m^{-3} HCl (HCl : NaCl = 0.1 : 1) yields a predicted aerosol composition with activities of 6.6 mol L^{-1} for $Cl^-_{(aq)}$ and 2.3 mol L^{-1}

for $H^+_{(aq)}$ (equivalent to a pH of −0.3) for RH = 76 %. As might be expected, acidification of $NaCl_{(aq)}$ aerosol by HCl leads to an increased acidity without causing a significant reduction in $Cl^-_{(aq)}$ concentration through acid-displacement (given the use of HCl as the acidifying agent).

On HCl-acidified $NaCl_{(aq)}$ aerosol, Abbatt and Wachewsky (1998) measured the uptake coefficient of HOBr to be > 0.2. We calculate the uptake coefficient for $HOBr + Cl^-$ under these experimental conditions, assuming a temperature of 298 K, a chloride concentration of 6.6 M on particles of 1 µm radius using both our new parameterisation for k^{II} and the termolecular approach to $HOBr + Cl^-$ kinetics. Both the approaches to calculating the uptake coefficient on HCl-acidified aerosol predict an $\gamma_{HOBr+Cl} \sim 0.6$, thus are consistent with the experimental findings, see the comparison in Table 4.

4.4.3 Low uptake coefficient on H_2SO_4-acidified sea-salt aerosol with RH dependence

From their measured uptake coefficients, Pratte and Rossi (2006) derived first-order rate constants for the reaction of $HOBr_{(aq)}$ finding $k^I \sim 10^3\,s^{-1}$. We used these data together with the E-AIM to derive k^{II} estimates from reported k^I, and also to investigate the RH-dependence of the reported uptake coefficients.

E-AIM model III calculations were performed for H_2SO_4-acidified sea-salt aerosol at $H_2SO_4 : NaCl = 1.45 : 1$, and 50 and 80 % RH, to predict aerosol composition under the experimental conditions of Pratte and Rossi (2006), where the E-AIM model III temperature of 298.15 K is close to the reported experimental conditions of 296 K. An estimated sea-salt concentration of 8 $\mu mol\,m^{-3}$ Na was assumed, based on the product of the NaCl molarity (e.g. 2.9 M at 70 % RH) initially estimated by Pratte and Rossi (2006) and the reported measured aerosol volume density ($2.7 \times 10^{-9} cm^3\,cm^{-3}$). To reach the reported experimental $H_2SO_4 : NaCl = 1.45 : 1$, an additional 11.6 $\mu M\,m^{-3}$ H_2SO_4 was added to the E-AIM input. For simplicity the same input estimate is used for E-AIM calculations across all RH.

Title Page
Abstract Introduction
Conclusions References
Tables Figures
◀| |▶
◀ ▶
Back Close
Full Screen / Esc
Printer-friendly Version
Interactive Discussion

The output of our E-AIM calculations gives good general agreement between the predicted E-AIM aerosol volume density (e.g. 0.67×10^{-9}, 2.2×10^{-9} and $5.5\times10^{-9}\,\mathrm{cm^3\,cm^{-3}}$ at RH = 40, 70 and 90 %, respectively) to that reported from their experimental observations (1.01×10^{-9}, 2.7×10^{-9} and $5.56\times10^{-9}\,\mathrm{cm^3\,cm^{-3}}$ at RH = 40, 70 and 90 %, respectively). However, the E-AIM data suggest the aerosol composition differs to that estimated by Pratte and Rossi (2006).

The E-AIM model predicts that $\mathrm{Cl^-_{(aq)}}$ concentrations are 6.8×10^{-10} and $1.5\times10^{-7}\,\mathrm{mol\,m^{-3}}$ at 50 and 80 % RH respectively, equivalent to $0.004\,\mathrm{M\,L^{-1}}$ and $0.08\,\mathrm{M\,L^{-1}}$. The corresponding $\mathrm{HCl_{(g)}}$ concentrations are 8.0 and 7.9 µmoles $\mathrm{m^{-3}}$. Thus, E-AIM predicts that the addition of $\mathrm{H_2SO_{4\,(aq)}}$ causes substantial acid-displacement of $\mathrm{HCl_{(g)}}$ from the sea-salt under the experimental conditions. The $\mathrm{HCl_{(g)}}$ displacement acts to lower the aerosol $\mathrm{Cl^-_{(aq)}}$ concentration, and the effect is more pronounced at low relative humidity where wt% $\mathrm{H_2SO_4}$ of the acidic aerosol solution is higher, hence HCl solubility lower.

Pratte and Rossi (2006) did not measure aerosol composition during their experiment, but make the assumption that chloride remained entirely in the aerosol-phase in their discussion of their data, noting that they not detect any $\mathrm{HCl_{(g)}}$. However, the predicted $\mathrm{HCl_{(g)}}$ concentrations by E-AIM e.g. $\sim 8\times10^{-6}\,\mathrm{mol\,m^{-3}}$, equivalent to $\sim 5\times10^{12}\,\mathrm{molec\,cm^{-3}}$ are below the $\sim 2\times10^{13}\,\mathrm{molec\,cm^{-3}}$detection limit reported by Pratte and Rossi (2006). This can also be shown directly from the aerosol properties estimated by Pratte and Rossi (2006). For example, at the reported aerosol volume of $2.7\times10^{-9}\,\mathrm{cm^3\,cm^{-3}}$ at 70 % RH would yield a maximum $\mathrm{HCl_{(g)}}$ concentration if HCl exsolution from the (estimated) $2.9\,\mathrm{M\,L^{-1}}$ NaCl concentration was complete, of $2.9\times10^{-3}\cdot2.7\times10^{-9}\cdot(6.023\times10^{23}) = 4.7\times10^{12}\,\mathrm{molec\,cm^{-3}}$, i.e. below their reported detection limit.

In the following, we show the depletion of chloride due to HCl-displacement reactions in $\mathrm{H_2SO_4}$-acidified sea-salt aerosol (as predicted by E-AIM) to be a plausible explanation for the low uptake coefficients for HOBr + Cl^- on this experimental aerosol, and the reported RH dependence.

On H_2SO_4-acidified sea-salt aerosol, Pratte and Rossi (2006) measured the uptake coefficient of HOBr to be $\sim 10^{-2}$ at H_2SO_4 : NaCl = 1.45 : 1, with an RH-dependence (finding $\gamma_{HOBr} \sim 10^{-3}$ at RH < 70 %). Using our parameterisation, we calculate the uptake coefficient for HOBr + Cl^- under these experimental conditions, at 298 K, and with variable RH. We assume a solubility of HOBr in sulphuric acid of 363 M atm^{-1} at 296 K (following Pratte and Rossi, 2006 based on Iraci et al., 2005), and calculate a HOBr rate constant of diffusion in sulphuric acid of 5.5×10^{-6} and 1.0×10^{-5} at 50 and 80 % RH (48 and 29 wt%H_2SO_4) respectively. We assume the abovementioned $Cl^-_{(aq)}$ concentrations predicted by E-AIM (0.004 M L^{-1} and 0.08 M L^{-1} at 50 and 80 % RH respectively), see Table 4.

Our new parameterisation for k^{II} yields uptake coefficients for HOBr+Cl^- of 4.4×10^{-3} at 50 % RH and 7.6×10^{-2} at 80 % RH, in broad agreement to the low uptake coefficients reported by Pratte and Rossi (2006); 1.0 ± 10^{-2} at RH ≥ 76 %. Such agreement is to some extent not surprising, given the usage of k^I reported at RH = 77–90 % from the same Pratte and Rossi (2006) experiments to derive an estimate for k^{II} at acid saturation (Fig. 1). Nevertheless, the uptake calculations confirm and provide a first explanation for the RH dependence of the uptake coefficient as reported by Pratte and Rossi (2006). The model indicates that the underlying cause of this trend is greater $[Cl^-_{(aq)}]$ at higher RH, given higher solubility of HCl at the lower wt%H_2SO_4 at high RH. This is further shown by Fig. 3 that compares the modelled and observed RH dependence of the uptake coefficient of HOBr across all reported data from 40–90 % RH, demonstrating broad agreement in the trend (noting discrepancies may result from impurities within the sea-salt solution or uncertainties within the parameterisations used in the uptake model).

We contrast these findings to the the termolecular approach to k^I that yields an uptake coefficient of 0.6 at both RH values, substantially overestimating γ_{HOBr} (by at least a factor of 20). This is because the termolecular approach assumes acid-dependent k^{II} across all pH, leading to an extremely high rate constant for the reaction of $HOBr + Cl^-$ at pH −1 to 0, and a very fast rate of reaction of HOBr with Cl^-: even though Cl^- concentrations are depleted by acid-displacement, the assumed increased rate constant at low pH overcompensates for this effect.

In conclusion, our new k^{II} parameterisation for the kinetics of $HOBr + X^-$ yields uptake coefficients in agreement with reported laboratory data, and – for the first time – reconciles differences between reported uptake on HCl-acidified and H_2SO_4-acidified sea-salt aerosols, within a single framework.

5 Atmospheric implications for BrO chemistry in the marine and volcanic environments

5.1 Declining uptake coefficients on progressively H_2SO_4-acidified sea-salt aerosol

Using our revised HOBr reaction kinetics (Fig. 1), we now re-evaluate the $HOBr + Br^-$ and $HOBr + Cl^-$ reactive uptake coefficients on a model sea-salt aerosol that undergoes progressive H_2SO_4-acidification and compare to calculations using the termolecular approach (Fig. 4). We investigate how the reductions in halide ion concentrations caused by the $H_2SO_{4\,(aq)}$ addition (through both acid-displacement reactions that deplete $[Cl^-_{(aq)}]$, and dilution of $[Br^-_{(aq)}]$ by $H_2SO_{4\,(aq)}$ volume, see Fig. 2) impact γ_{HOBr} at low pH.

We assume a particle radius of 1 or 0.1 µm in the uptake calculation. Temperature is set to 298 K and RH = 80 % (above deliquesence). For aerosol that is alkaline or only weakly acidic (pH 12 to pH 4), uptake coefficients were calculated assuming a fixed sea-salt composition with $[Cl^-_{(aq)}] = 5.3$ M and $[Br^-_{(aq)}] = 0.008$ mol L^{-1}, with pH varied between 4 and 12 (E-AIM was not used given very low degree of H_2SO_4-acidification). For more strongly acidified sea-salt, across H_2SO_4 : Na ratios from 0.05 to 400 (pH 4 to −0.87 for the model aerosol conditions), E-AIM was used to determine the extent of acid-displacement of HCl from acidified $NaCl_{(aq)}$ aerosol, with aerosol $Br^-_{(aq)}$ determined using an effective Henry's law solubility for HBr (see predicted composition in Fig. 2).

Figure 4 shows the calculated reactive uptake for $HOBr + Br^-$ and $HOBr + Cl^-$ increase with increasing acidity over pH 4–12 for the uptake coefficient for 0.1 and 1 µm radius particles, similar to that previously reported using the termolecular approach. The alkaline to acid transition in γ_{HOBr} reflects the increase in the underlying $HOBr_{(aq)}$ k^I rate constant with acidity due to the onset of the acid assisted mechanism, Fig. 1 as well as the decrease of HOBr partitioning to BrO^-. $\gamma_{HOBr+Cl}$ reaches values close to the accommodation limit by pH ≤ 8 (for 1 µm radius particles) or pH ≤ 7 (for 0.1 µm radius particles) while $\gamma_{HOBr+Br}$ reaches values close to the accommodation limit by pH ≤ 5 (for 1 µm radius particles) or pH ≤ 4 (for 0.1 µm radius particles).

In the high acidity regime, the acid-saturation of k^{II} can cause γ_{HOBr} to plateau at a level slightly lower than α (e.g. in $\gamma_{HOBr+Cl}$ at pH ∼ 4), in contrast to the termolecular approach. Overall, for slightly-acidified sea-salt aerosol, reactive uptake of HOBr is driven primarily by $\gamma_{HOBr+Cl}$. $\gamma_{HOBr+Br}$ reaches similar values to $\gamma_{HOBr+Cl}$ at pH ∼ 3–4 for the specific model aerosol conditions of this study.

However, as the degree acidification by H_2SO_4 increases, the uptake coefficient for $HOBr + Cl^-$ begins to decline at pH < 4. This is due to acid-displacement reactions that convert $Cl^-_{(aq)}$ into $HCl_{(g)}$, thereby lowering $[Cl^-_{(aq)}]$. This leads to $\gamma_{HOBr+Cl^-} < \gamma_{HOBr+Br-}$, i.e. HOBr reactive uptake becomes driven by $HOBr + Br^-$ below a pH of ∼ 2 for the specific aerosol conditions of this study. As H_2SO_4 : Na ratio increases further and pH decreases further, the uptake coefficient for $HOBr + Br^-_{(aq)}$ also begins to decline. This is principally due to the dilution of $Br^-_{(aq)}$ by the additional volume of $H_2SO_{4\,(aq)}$ that becomes important particularly at very high H_2SO_4 : Na.

Notably, the declines in uptake coefficients are greatest for smaller particles, for which there is a greater probability that $HOBr_{(aq)}$ may diffuse across the particle and be released to the gas phase, without any aqueous-phase reaction occurring.

The uptake coefficients are also further reduced if parameterisations for the solubility of HOBr in $H_2SO_{4\,(aq)}$ is assumed in the uptake equation rather than that for water. The exact point of transition between these two parameterisations is not well constrained, but it is clear that the $H_2SO_{4\,(aq)}$ parameterisations become more applicable than water with greater acidification, and must certainly be more relevant at high H_2SO_4 : Na e.g. at 400 : 1. The lower solubility of HOBr in $H_2SO_{4\,(aq)}$ acts to decrease the uptake coefficient, and is found to have a stronger impact on γ_{HOBr} than the slower rate of diffusion of $\mathrm{HOBr}_{(aq)}$ in H_2SO_4.

In summary, following a rise over the alkaline-acid transition, our revised HOBr kinetics yields HOBr reactive uptake coefficients that subsequently decline on progressively H_2SO_4-acidified sea-salt aerosol. For the aerosol concentration assumed, the uptake coefficient on the 0.1 µm radius particles declines to $\gamma_{\mathrm{HOBr+Br}} < 0.03$ at a H_2SO_4 : Na ratio of 400 : 1, indicating that the reactive uptake of HOBr on highly acidified submicrometer particles is extremely low, Fig. 4. These decreases in uptake coefficient with increasing aerosol acidity are not captured by calculations that assume termolecular kinetics. As stated in the previous section, this is because the termolecular approach assumes the HOBr rate constant is acid-dependent across all pH, and does not consider acid-saturation of the rate constant.

We note that $H^+_{(aq)}$ is consumed in the reaction, therefore a source of acidity is required to sustain prolonged BrO formation chemistry. However, the γ_{HOBr} dependency on acidity shown here suggests that excessive aerosol acidification by $H_2SO_{4\,(aq)}$ exerts a limitation on the extent of reactive bromine formation via HOBr uptake, particularly for small particle sizes. Further implications for BrO chemistry in the marine boundary layer are now discussed.

5.2 Reduced BrO cycling in the marine boundary layer (MBL)

The MBL typically contains a multi-modal aerosol size distribution, including slightly acidic supra-micron particles and substantially acidified submicron particles (e.g. Keene et al., 2002). Whilst fresh sea-salt aerosol is alkaline, acids of natural or anthropogenic origin, such as H_2SO_4 or HNO_3 may interact with the aerosol with acid-displacement reactions leading to release of $HCl_{(g)}$ and depletion of aerosol $Cl^-_{(aq)}$. The $HCl_{(g)}$ released acts as a gas-phase reservoir of acidity (Von Glasow and Sander, 2001). Observations find that the sub-micron particles are typically highly acidified by $H_2SO_{4\,(aq)}$, and thus contain relatively low concentrations of sea-salt components. $Cl^-_{(aq)}$ is depleted in these particles. The supra-micron particles are acidified to a lesser extent, but can also exhibit a degree of chloride-depletion. For example, Keene et al. (2002) report aerosol pH in Bermuda in 1997 under moderately polluted conditions of pH 3–4 for supramicron sized particles, and pH 1–2 for finer sized fractions, with all particle pH buffered by the $H^+ + SO_4^{2-} \leftrightarrow HSO_4^-$ equilibrium. Sulfate dominated the submicrometer size fraction, for example $Na < 2.4\,\mathrm{nmol\,m^{-3}}$ for the 0.3 µm diameter particles sampled whilst the maximum $SO_4^{2-} \sim 69.8\,\mathrm{nmol\,m^{-3}}$ and median $SO_4^{2-} = 5.93\,\mathrm{nmol\,m^{-3}}$.

To date, it has been assumed that HOBr reactive uptake is rapid on both the sub- and supra-micron fractions of acidified marine aerosol (e.g. Sander et al., 2003). However, our re-evaluation of HOBr reactive kinetics (Fig. 1) indicates HOBr reactive uptake to be low on the highly-acidified sub-micron particles ($\gamma_{\mathrm{HOBr}} < 0.03$). Thus the contribution of the submicron aerosol fraction to HOBr uptake is much smaller than has been assumed to date.

Furthermore, a negative feedback exists in the reactive uptake of $\mathrm{HOBr} + \mathrm{Br}^-$ as the BrO formation chemistry progresses: given $\gamma_{\mathrm{HOBr+Br}}$ is a function of $[Br^-_{(aq)}]$, the conversion of $Br^-_{(aq)}$ to $Br_{2\,(g)}$ acts to decrease aerosol $[Br^-_{(aq)}]$, reducing subsequent values of $\gamma_{\mathrm{HOBr+Br}}$. As already mentioned, $\gamma_{\mathrm{HOBr+Cl}}$ is reduced on H_2SO_4-acidified (Cl^--depleted) sea-salt aerosol, such that uptake is driven by $\mathrm{HOBr} + \mathrm{Br}^-$, Fig. 4. Therefore this negative feedback for $\gamma_{\mathrm{HOBr+Br}}$ will play a much more significant role for overall HOBr reactive uptake according our revised HOBr kinetics than has been assumed by model studies to date.

We suggest both of the abovementioned factors (the reduced uptake coefficient on highly-acidified sea-salt particles, and the HOBr + Br^- negative-feedback) as potential underlying reasons for the over-prediction by numerical models of BrO cycling in the marine environment (Sander et al., 2003; Smoydzin and von Glasow, 2007; Keene et al., 2009). Inclusion of the new HOBr kinetics into such models will allow our hypothesis to be tested and quantified.

5.3 A first-explanation for Br-enriched sub-micron aerosol in the marine environment

An atmospheric phenomenon that is observed to be relatively widespread but has not previously been explained is the occurrence of Br-enrichment in highly acidified sub-micron sea-salt particles simultaneous to Br-depletion in supramicron sea-salt particles, see Sander et al. (2003) and references therein. For example, inorganic aerosol bromine depletion often exceeds 50 % in the supramicron particle size fraction whereas bromide enrichment may reach 10's % in the submicrometer fraction. Whilst reactive halogen chemistry can readily explain the occurrence of Br-depletion in sea-salt aerosols, a review by Sander et al. (2003) asks the open question "How can bromine accumulate in submicrometer particles instead of being recycled back into the gas phase?".

From Fig. 4, we can propose a mechanism for Br-enrichment. The acidified supramicron particles support reactive uptake of HOBr, with release of reactive bromine leading to Br-depletion in these particles. However, HOBr uptake coefficients on the highly-acidified sub-micron particles are low: the HOBr + Cl^- coefficient is reduced due to acid-displacement of $HCl_{(g)}$ and the HOBr + Br^- coefficient is reduced due to dilution of $[Br^-_{(aq)}]$ at high H_2SO_4 : Na ratios (note that Na is also diluted so does not change relative Br : Na, or the Br^- enrichment factor). Thus there is a high overall probability that $HOBr_{(aq)}$ diffuses across and out of the sub-micrometer particles without reaction occurring, yielding low γ_{HOBr}. As consequence, the submicron particles do not readily become depleted in $Br^-_{(aq)}$. Moreover, the release of $Br_{2(g)}$ from the supra-micron particles leads to the continual formation of gas-phase reactive bromine species (such as BrO) in the MBL, of which a proportion will be converted to $HBr_{(g)}$ (e.g. via reaction of Br with HCHO, or reaction of BrO with OH). Deposition of gas-phase bromine species like HBr to the submicron aerosol yields a source of $Br^-_{(aq)}$. The net effect is for $Br^-_{(aq)}$ concentrations to become enhanced (relative to Na) in the sub-micron aerosol simultaneous to becoming depleted in the supra-micron aerosol. Note that this argumentation is only possible using our new uptake calculations based on k^{I} calculated using revised HOBr kinetics in terms of k^{II} as the termolecular approach predicts high HOBr uptake for both particle types. We encourage our new rate constants calculations for HOBr reactive uptake to be incorporated into numerical models to test and quantify submicron aerosol Br-enrichment via our proposed mechanism.

5.4 Reactive uptake of HOBr on volcanic aerosol

HOBr reactive uptake coefficients are now calculated for the first time onto aerosol in a halogen-rich volcano plume, using the k^{II} parameterisations for $HOBr + Br^-$ and $HOBr + Cl^-$, and E-AIM predictions of the volcanic aerosol composition.

The predicted aerosol and plume composition for Etna is shown in Fig. 5 for two of the three plume dilution scenarios, at three different temperatures. Whilst the Etna emission $((SO_2) : HCl : H_2SO_4 : HBr$ at molar ratios $1 : 0.5 : 0.01 : 0.00075)$ contains substantially less HBr than HCl, the higher solubility of HBr relative to HCl leads to relatively similar aqueous-phase concentrations for $Cl^-_{(aq)}$ and $Br^-_{(aq)}$. Both aqueous-phase halide concentrations are more elevated in the stronger ($30\,\mu mol\,m^{-3}$ SO_2) plume than the dilute ($0.3\,\mu mol\,m^{-3}$ SO_2) plume scenarios as a consequence of the greater HX partial pressures promoting gas-to-aerosol partitioning in the concentrated plume scenario. Temperature exerts a significant control on $[X^-_{(aq)}]$ through the inverse dependence of halide solubility on temperature. Relative humidity (RH) also exerts a control on $[X^-_{(aq)}]$:

the dependence of $[X^-_{(aq)}]$ on RH is initially positive, as HX solubility is greater at higher pH (thus, higher RH). However, in the more concentrated plume scenario the increase in aerosol volume with RH can lead to complete removal of $HX_{(g)}$ followed by dilution of $[X^-_{(aq)}]$. The decline in $[X^-_{(aq)}]$ is more pronounced and occurs earlier for $Br^-_{(aq)}$ than $Cl^-_{(aq)}$ given higher solubility and lower gas-phase concentrations. These declines in $[X^-_{(aq)}]$ are only seen for the strong plume scenario as gas-to-aerosol partitioning is much lower for the dilute plume scenario such that HX is not depleted. The Br^- composition used here for Etna is based on an average volcanic Br/S emission reported by Aiuppa et al. (2006), as used in the modelling study of Roberts et al. (2013), and a factor of two and three lower than that assumed by Roberts et al. (2009) and von Glasow (2010) respectively. Our assumed volcanic aerosol composition also differs to that reported by Martin et al. (2012) in an E-AIM study of the Masaya volcano emission, due to differences in the volcano-specific gas and aerosol emission, although both of our E-AIM applications predict similar tendencies for aerosol compositional changes as a function of temperature and RH.

Using the volcanic aerosol composition predicted by E-AIM, uptake coefficients for HOBr+Br and HOBr+Cl are calculated across tropospheric temperature and relative humidity, for three different plume dilutions (30, 3 and 0.3 $\mu mol\,m^{-3}$, which are equivalent to ~ 1 ppmv, 0.1 ppmv, and 0.01 ppmv SO_2 at 4 km altitude in US standard atmosphere), and assuming a particle radius of 1 µm, Fig. 6. Also shown is the uptake coefficient for an evolved volcanic plume composition, where it is assumed a substantial conversion of $Br^-_{(aq)}$ to reactive bromine has occurred. There exists no experimental information regarding the temperature dependence of k^{II} for HOBr + X. Here it is assumed the variation k^{II} with temperature over 230–300 K is small compared to the temperature dependence of the HOBr and HX solubilities (which vary by several orders of magnitude over the parameter space).

High HOBr uptake coefficients are predicted at low tropospheric temperatures: $\gamma_{HOBr+Br^-} \approx \gamma_{HOBr+Cl^-} \approx 0.6$. The uptake coefficient decreases markedly with increasing temperature for $\gamma_{\mathrm{HOBr+Cl^-}}$ and also decreases for $\gamma_{\mathrm{HOBr+Br^-}}$ in the most dilute plume scenario. The inverse temperature trend in γ_{HOBr} (particularly for $\gamma_{\mathrm{HOBr+Cl}}$) is caused by a lower solubility of HCl in sulphuric acid particles at higher tropospheric temperatures, augmented by a similar temperature trend in the solubility of $\mathrm{HOBr_{(aq)}}$. The variation with plume dilution is explained by the fact that lower gas-to-aerosol partitioning yields lower $[\mathrm{X^-_{(aq)}}]$ in the dilute plume scenarios thus a lower $k^{\mathrm{I}} = k^{\mathrm{II}} \cdot [\mathrm{X^-_{(aq)}}]$ in the uptake equation, hence a reduced γ_{HOBr}.

Figure 6 also illustrates a weak dependence of the uptake coefficients on relative humidity, due to increasing solubility of the halides with RH or lower wt%$\mathrm{H_2SO_4}$ (see Fig. 5 and Sect. 3.7, any RH-dependence of HOBr solubility not considered here, see Methods). As for the marine aerosol study, reductions in γ_{HOBr} are more pronounced for particles of smaller radii (data not shown), as the probability for diffusion across the particle without reaction is higher. According to Fig. 6, $\gamma_{\mathrm{HOBr+Br}}$ is equal to or exceeds $\gamma_{\mathrm{HOBr+Cl}}$ under all temperature and humidity scenarios for the composition of the Etna emission. This is driven by the greater k^{II} for $\mathrm{HOBr + Br^-}$, and the higher solubility of HBr compared to HCl. However, the evolved plume scenario where it is assumed $\mathrm{Br^-_{(aq)}}$ concentrations reduced (as consequence of reactive bromine release to the gas phase) yields a much lower uptake coefficient for $\mathrm{HOBr + Br^-}$.

As in the case of sea-salt aerosol, uptake coefficient calculations using the k^{II} parameterisation differ markedly from that calculated using the termolecular approach to HOBr kinetics which yields high and typically accommodation limited HOBr uptake coefficients throughout the parameter space (also shown in Fig. 6).

5.5 Implications for reactive halogen chemistry in volcano plumes

We conclude that important factors governing the HOBr reactive uptake coefficient in volcanic plumes are: plume composition (particularly halogen : sulphate ratios), plume strength or dilution (through its effect on halogen gas-aerosol partitioning), aerosol size, ambient temperature and relative humidity, for which the emission altitude and season exert primary controls. The overall rate of reactive uptake of HOBr in a volcano plume depends also on the concentration of $HOBr_{(g)}$ and aerosol surface area density, as well as the uptake coefficient (see Eq. 1).

Figure 6 shows that in concentrated plumes near to the volcanic source, the aqueous-phase halide concentrations are sufficiently high that $\gamma_{HOBr+Br}$ is accommodation-limited. Rapid formation of BrO is expected to occur. This is consistent with observations of volcanic BrO at numerous volcanoes globally (e.g. Bobrowski et al., 2007b; Boichu et al., 2011, and references therein), including emissions from both low and high altitude volcanoes.

As the volcanic plume disperses into the troposphere the HOBr gas and aerosol concentration (hence surface area density) decline. Therefore the rate of HOBr reactive uptake is expected to decline with plume dilution, which is further reinforced by the predicted decline in γ_{HOBr} as the plume disperses and dilutes, particularly for $\gamma_{HOBr+Cl}$, which is low at temperatures representative of the lower troposphere. As a result of this decline, the HOBr reactive uptake becomes driven by $\gamma_{HOBr+Br}$ in dispersed plumes under most tropospheric conditions, and in low-altitude plumes. Under these circumstances a negative feedback exists as BrO chemistry progresses: the conversion of $Br^-_{(aq)}$ to $Br_{2\,(g)}$acts to deplete $[Br^-_{(aq)}]$, and consequently reduces the $HOBr + Br^-$ uptake coefficient, as shown in Fig. 6 for the evolved plume scenario (with maximum possible $Br^-_{(aq)}$ depletion).

These reductions in $\gamma_{HOBr+Br}$ and $\gamma_{HOBr+Cl}$ with plume dispersion and chemical evolution will act to slow the rate of reactive bromine cycling in the dispersed plume. However, for plumes injected into the mid-upper troposphere, at low ambient temperatures (hence high solubility for HOBr, and HX and low rate of diffusion of $HOBr_{(aq)}$), γ_{HOBr} values remain relatively high. Therefore continued BrO cycling in the downwind plumes from eruptions into the mid-troposphere (e.g. Eyjafjallajökull) or in plumes from quiescently degassing volcanoes with elevated summits (e.g. Etna, Italy, ~ 3.3 km a.s.l.) is expected. For volcanoes emitting at low altitudes at high ambient tropospheric temperatures, BrO cycling is expected to be initially rapid (given high plume gas and aerosol concentrations as well as high $\gamma_{\mathrm{HOBr+Br}}$), but the decreased uptake coefficient in the dispersed plume may limit the extent of BrO cycling further downwind.

To date, numerical model studies of the impacts of volcanic halogens reactive halogen chemistry in the troposphere have either used a fixed uptake coefficient (Roberts et al., 2009, 2013; Kelly et al., 2013) or the termolecular approach to HOBr kinetics (Bobrowski et al., 2009; von Glasow, 2010). Figure 6 illustrates both of these approaches will lead to modelling inaccuracies, particularly in the downwind plume. We recommend incorporation of more realistic HOBr kinetics in these models, using the parameterisations proposed here, in order to accurately simulate the reactive bromine chemistry and plume impacts.

6 Conclusions

This study introduces a new evaluation of HOBr reactive uptake coefficients on aerosol of different compositions, in the context of the general acid assisted mechanism. We emphasise that the termolecular kinetic approach assumed in numerical model studies of tropospheric reactive bromine chemistry to date is strictly only valid for a specific pH range. Rather, according to the general acid assisted mechanism, the reaction kinetics for HOBr becomes independent of pH at high acidity. By re-evaluation of reported rate constant data from uptake experiments on acidified sea-salt aerosol, and consideration of relative reaction rates according to nucleophile strength, we identify the kinetics of $\mathrm{HOBr + Cl^-}$ may saturate below pH 6 to yield a second-order rate constant of $k^{\mathrm{II}} \sim 10^4\,\mathrm{M\,s^{-1}}$. The kinetics of $\mathrm{HOBr{+}Br^-}$ saturates at $k^{\mathrm{II}} \sim 10^8$–$10^9\,\mathrm{M\,s^{-1}}$ at pH $<\sim 1$ based on experimental data and kinetics estimates of Eigen and Kustin (1962) and Beckwith et al. (1996).

This study reconciles for the first time the different reported uptake reactive coefficient from laboratory experiments. The new k^{II} parameterisation yields uptake coefficients that are consistent with reported uptake experiments: $\gamma_{\mathrm{HOBr}} = 0.6$ on supersaturated NaBr aerosol (Wachsmuth et al., 2002); $\gamma_{\mathrm{HOBr}} > 0.2$ on HCl-acidfied sea-salt aerosol (Abbatt and Wachsewsky, 1998), $\gamma_{HOBr} = 10^{-2}$ on H_2SO_4-acidifed sea-salt aerosol, with an RH dependence (Pratte and Rossi, 2006). The variation in uptake coefficient across the alkaline-aerosol transition is similar to that previously predicted using the termolecular approach but uptake calculations using our revised kinetics of HOBr show much lower uptake coefficients for HOBr in highly acidified sea-salt aerosol, particularly for small particle radii. This is due to acid-displacement of $HCl_{(g)}$ at high acidity slowing the rate of reaction of HOBr + Cl^-, thus lowering $\gamma_{HOBr+Cl}$, with dilution of $[Br^-_{(aq)}]$ at very high H_2SO_4 : sea-salt ratios slowing the rate of reaction of HOBr + Br^-, thus lowering $\gamma_{HOBr+Br}$. This finding is in contrast to previous uptake calculations that assumed high γ_{HOBr} at high acidity based on termolecular reaction kinetics in which k^{II} increases with acidity and which overcompensates for the decrease in halide concentration with increasing acidity. Thus, the termolecular approach, as currently used in numerical models of tropospheric BrO chemistry, may cause HOBr reactive uptake to be substantially over estimated in aerosol at high acidity.

Implications for BrO chemistry in the marine boundary layer have been discussed. The HOBr uptake coefficient is predicted to be high on slightly acidified supra-micron particles but extremely low on highly-acidified sub-micron particles. A first explanation for the observed Br-enrichment in the sub-micron particles simultaneous to Br-depletion in supra-micron particles is thereby proposed, as reactive bromine release from the supra-micron fraction may deposit and accumulate in the submicron fraction, that does not undergo significant Br^- depletion. Because the HOBr + Br^- uptake coefficient is a function of $Br^-_{(aq)}$ concentrations, a negative feedback can occur as the marine BrO chemistry evolves, and supramicron particle $Br^-_{(aq)}$ concentrations are lowered by the release of reactive bromine. According to our revised HOBr kinetics (yielding $\gamma_{HOBr+Br^-} > \gamma_{HOBr+Cl^-}$), this negative feedback for $\gamma_{HOBr+Br^-}$ exerts a stronger overall influence on the rate of HOBr reactive uptake than previous studies have assumed.

Calculations on volcanic aerosol show that uptake is high and accommodation limited in the concentrated near-source plume, enabling BrO formation to rapidly occur.

Uptake coefficients are reduced in more dilute plumes, particularly for HOBr + Cl^-, at high temperatures, for small particle radii, and for HOBr + Br^- in evolved plume composition scenarios. The findings suggest that HOBr uptake on sulphate aerosol directly emitted from volcanoes can readily promote BrO cycling in plumes dispersing into the upper or middle troposphere (quiescently degassing from elevated volcano summits e.g. Etna, or explosive eruptions e.g. Eyjafjallajökull). BrO cycling may be reduced by low uptake coefficients in the dispersed downwind plume, particularly at higher tropospheric temperatures (low altitude emissions). Inclusion of our revised HOBr reaction kinetics in numerical models of volcanic plume chemistry (or uptake coefficients derived therefrom) is required to accurately predict the impacts of volcanic halogens on the troposphere.

Acknowledgements. T. J. Roberts and L. Jourdain are grateful for funding from LABEX VOLTAIRE (VOLatils-Terre Atmosphère Interactions – Ressources et Environnement) ANR-10-LABX-100-01 (2011–20). PTG acknowledges the ERC for funding.

References

Abbatt, J. P. D. and Waschewsky, G. C. G.: Heterogeneous interactions of HOBr, HNO_3, O_3, and NO_2 with deliquescent NaCl aerosols at room temperature, J. Phys. Chem. A, 102, 3719–3725, 1998.

Ammann, M., Cox, R. A., Crowley, J. N., Jenkin, M. E., Mellouki, A., Rossi, M. J., Troe, J., and Wallington, T. J.: Evaluated kinetic and photochemical data for atmospheric chemistry: Volume VI – heterogeneous reactions with liquid substrates, Atmos. Chem. Phys., 13, 8045–8228, doi:10.5194/acp-13-8045-2013, 2013.

Barrie, L. A., Bottenheim, J. W., Schnell, R. C., Crutzen, P. J., and Rasmussen, R. A.: Ozone destruction and photochemical reactions at polar sunrise in the lower Arctic atmosphere, Nature, 334, 138–141, 1998.

Beckwith, R. C., Wang, T. X., and Margerum, D. W.: Equilibrium and kinetics of bromine hydrolysis, Inorg. Chem., 35, 995–1000, 1996.

Title Page
Abstract | Introduction
Conclusions | References
Tables | Figures
◀| |▶
◀ ▶
Back | Close
Full Screen / Esc
Printer-friendly Version
Interactive Discussion

Blatchley, E. R., Johnson, R. W., Alleman, J. E., and McCoy, W. F.: Effective Henry's law constants for free chlorine and free bromine, Water Res., 26, 99–106, 1991.

Bobrowski, N. and Platt, U.: SO_2/BrO ratios studied in five volcanic plumes, J. Volcanol. Geoth. Res., 166, 147–160, doi:10.1016/j.jvolgeores.2007.07.003, 2007.

Bobrowski, N., Honniger, G., Galle, B., and Platt, U.: Detection of bromine monoxide in a volcanic plume, Nature, 423, 273–276, doi:10.1038/nature01625, 2003.

Bobrowski, N., von Glasow, R., Aiuppa, A., Inguaggiato, S., Louban, I., Ibrahim, O. W., and Platt, U.: Reactive halogen chemistry in volcanic plumes, J. Geophys. Res., 112, D06311, doi:10.1029/2006JD007206, 2007.

Boichu, M., Oppenheimer, C., Roberts, T. J., Tsanev, V., and Kyle, P. R.: On bromine, nitrogen oxides and ozone depletion in the tropospheric plume of Erebus volcano (Antarctica), Atmos. Environ., 45, 3856–3866, 2011.

Breider, T. J., Chipperfield, M. P., Richards, N. A. D., Carslaw, K. S., Mann, G. W., and Spracklen, D. V.: Impact of BrO on dimethylsulfide in the remote marine boundary layer, Geophys. Res. Lett., 37, L02807, doi:10.1029/2009GL040868, 2010.

Carslaw, K. S., Clegg, S. L., and Brimblecombe, P.: A thermodynamic model of the system HCl–HNO_3–H_2SO_4–H_2O, including solubilities of HBr, from < 200 K to 328 K, J. Phys. Chem., 99, 11557–11574, 1995.

Clegg, S. L., Brimblecombe, P., and Wexler, A. S., A thermodynamic model of the system H^+–NH_4^+-Na^+-SO_4^{2-}–NO_3^-–Cl^-–H_2O at 298.15 K, J. Phys. Chem. A, 102, 2155–2171, 1998.

Eigen, M. and Kustin, K.: The kinetics of halogen hydrolysis, J. Am. Chem. Soc., 1962, 1355–1361, doi:10.1021/ja00867a005, 1962.

Fickert, S., Adams, J. W., and Crowley, J. N.: Activation of Br_2 and BrCl via uptake of HOBr onto aqueous salt solutions, J. Geophys. Res., 104, 23719–23727, 1999.

Frenzel, A., Scheer, V., Sikorski, R., George, C., Behnke, W., and Zetzsch, C.: Heterogenerous interconversion reactions of $BrNO_2$, $ClNO_2$, Br_2, and Cl_2, J. Phys. Chem. A, 102, 1329–1337, 1998.

Gerritsen, C. M. and Margarem, D. W.: Non-metal redox kinetics: hypochlorite and hypochlorous acid reactions with cyanide, Inorg. Chem., 29, 2757–2762, 1990.

Iraci, L. T., Michelsen, R. R., Ashbourn, S. F. M., Rammer, T. A., and Golden, D. M.: Uptake of hypobromous acid (HOBr) by aqueous sulfuric acid solutions: low-temperature solubility and reaction, Atmos. Chem. Phys., 5, 1577–1587, doi:10.5194/acp-5-1577-2005, 2005.

Liu, Q. and Magarem, D. W.: Equilibrium and kinetics of bromine, Environ. Sci. Technol., 35, 1127–1133, 2001.

Keene, W. C., Pszenny, A. A. P., Maben, J. R., and Sander, R.: Variation of marine aerosol acidity with particle size, Geophys. Res. Lett., 29, 1101, doi:10.1029/2001GL013881, 2002.

Keene, W. C., Long, M. S., Pszenny, A. A. P., Sander, R., Maben, J. R., Wall, A. J., O'Halloran, T. L., Kerkweg, A., Fischer, E. V., and Schrems, O.: Latitudinal variation in the multiphase chemical processing of inorganic halogens and related species over the eastern North and South Atlantic Oceans, Atmos. Chem. Phys., 9, 7361–7385, doi:10.5194/acp-9-7361-2009, 2009.

Kelly P. J., Kern, C., Roberts, T. J., Lopez, T., Werner, C., and Aiuppa, A.: Rapid chemical evolution of tropospheric volcanic emissions from Redoubt Volcano, Alaska, based on observations of ozone and halogen-containing gases, J. Volcanol. Geoth. Res., 259, 317–333, 2013.

Klassen, J. K., Hu, Z., and Williams, L. R.: Diffusion coefficients for HCl and HBr in 30 wt % to 72 wt % sulfuric acid at temperatures between 220 and 300 K, J. Geophys. Res., 103, 16197–16202, 1998.

Kumar, K. and Margarem, D. W.: Kinetics and mechanism of general-acid-assisted oxidation of bromide by hypochlorite and hypochlorous acid, Inorg. Chem., 26, 2706–2711, 1987.

Martin, R. S., Wheeler, J. C., Ilyinskaya, E., Braban, C. F., and Oppenheimer, C.: The uptake of halogen (HF, HCl, HBr and HI) and nitric (HNO_3) acids into acidic sulphate particles in quiescent volcanic plumes, Chem. Geol., 296–297, 19–25, 2012.

Nagy, P. and Ashby, M. T.: Reactive sulfur species: kinetics and mechanisms of the oxidation of cysteine by hypohalous acid to give cysteine sulfenic acid, J. Am. Chem. Soc., 129, 14082–14091, 2007.

Nagy, J. C., Kumar, K., and Margarem, D. W.: Non-metal redox kinetics: oxidation of iodide by hypochlorous acid and by nitrogen trichloride measured by the pulsed-accelerated-flow method, Inorg. Chem., 27, 2773–2780, 1988.

Parrella, J. P., Jacob, D. J., Liang, Q., Zhang, Y., Mickley, L. J., Miller, B., Evans, M. J., Yang, X., Pyle, J. A., Theys, N., and Van Roozendael, M.: Tropospheric bromine chemistry: implications for present and pre-industrial ozone and mercury, Atmos. Chem. Phys., 12, 6723–6740, doi:10.5194/acp-12-6723-2012, 2012.

Pratte, P. and Rossi, M. J.: The heterogeneous kinetics of HOBr and HOCl on acidified sea salt and model aerosol at 40–90 % relative humidity and ambient temperature, Phys. Chem. Chem. Phys., 8, 3988–4001, 2006.

Read, K. A., Mahajan, A. S., Carpenter, L. J., Evans, M. J., Faria, B. V. E., Heard, D. E., Hopkins, J. R., Lee, L. D., Moller, S. J., Lewis, A. C., Mendes, L., McQuaid, J. B., Oetjen, H., Saiz-Lopez, A., Pilling, M. J., and Plane, J. M. C., Extensive halogen-mediated ozone destruction over the tropical Atlantic Ocean, Nature, 453, 1232–1235, doi:10.1038/nature07035, 2008.

Roberts, T. J., Braban, C. F., Martin, R. S., Oppenheimer, C., Adams, J. W., Cox, R. A., Jones, R. L., and Griffiths, P. T.: Modelling reactive halogen formation and ozone depletion in volcanic plumes, Chem. Geol., 263, 151–163, 2009.

Roberts, T. J., Martin, R. S., and Jourdain, L.: Reactive bromine chemistry in Mt Etna's volcanic plume: the influence of total Br, high temperature processing, aerosol loading and plume-air mixing, Atmos. Chem. Phys., submitted, 2013.

Saiz-Lopez, A. and von Glasow, R.: Reactive halogen chemistry in the troposphere, Chem. Soc. Rev., 41, 6448–6472, 2012.

Sander, R.: Compilation of Henry's Law Constants for Inorganic and Organic Species of Potential Importance in Environmental Chemistry (Version 3), available at: http://www.henrys-law.org (last access: November 2013), 1999.

Sander, R., Keene, W. C., Pszenny, A. A. P., Arimoto, R., Ayers, G. P., Baboukas, E., Cainey, J. M., Crutzen, P. J., Duce, R. A., Hönninger, G., Huebert, B. J., Maenhaut, W., Mihalopoulos, N., Turekian, V. C., and Van Dingenen, R.: Inorganic bromine in the marine boundary layer: a critical review, Atmos. Chem. Phys., 3, 1301–1336, doi:10.5194/acp-3-1301-2003, 2003.

Sander, R., Baumgaertner, A., Gromov, S., Harder, H., Jöckel, P., Kerkweg, A., Kubistin, D., Regelin, E., Riede, H., Sandu, A., Taraborrelli, D., Tost, H., and Xie, Z.-Q.: The atmospheric chemistry box model CAABA/MECCA-3.0, Geosci. Model Dev., 4, 373–380, doi:10.5194/gmd-4-373-2011, 2011.

Schroeder, W. H., Anlauf, K. G., Barrie, L. A., Lu, J. Y., Steffen, A., Schneeberger, D. R., and Berg, T.: Arctic springtime depletion of mercury, Nature, 394, 331–332, doi:10.1038/28530, 1998.

Schweizer, F., Mirabel, P., and George, C.: Uptake of hydrogen halides by water droplets, J. Phys. Chem. A, 104, 72–76, 2000.

Seinfeld, J. H. and Pandis, S. N.: Atmospheric Chemistry and Physics – from Air Pollution to Climate Change, 2nd edn., John Wiley & Sons, available at: http://www.knovel.com/web/portal/browse/display?_EXT_KNOVEL_DISPLAY_bookid=2126&VerticalID=0 (last access: November 2013), 2006.

Simpson, W. R., von Glasow, R., Riedel, K., Anderson, P., Ariya, P., Bottenheim, J., Burrows, J., Carpenter, L. J., Frieß, U., Goodsite, M. E., Heard, D., Hutterli, M., Jacobi, H.-W., Kaleschke, L., Neff, B., Plane, J., Platt, U., Richter, A., Roscoe, H., Sander, R., Shepson, P., Sodeau, J., Steffen, A., Wagner, T., and Wolff, E.: Halogens and their role in polar boundary-layer ozone depletion, Atmos. Chem. Phys., 7, 4375–4418, doi:10.5194/acp-7-4375-2007, 2007.

Smoydzin, L. and von Glasow, R.: Do organic surface films on sea salt aerosols influence atmospheric chemistry? – a model study, Atmos. Chem. Phys., 7, 5555–5567, doi:10.5194/acp-7-5555-2007, 2007.

Vogt, R., Crutzen, P. J., and Sander, R.: A mechanism for halogen release from sea-salt aerosol in the remote marine boundary layer, Nature, 383, 327–330, 1996.

Von Glasow, R.: Atmospheric chemistry in volcanic plumes, P. Natl. Acad. Sci. USA, 107, 6594–6599, 2010.

Von Glasow, R. and Sander, R.: Variation of sea salt aerosol pH with relative humidity, Geophys. Res. Lett., 28, 247–250, 2001.

Von Glasow, R., Sander, R., Bott, A., and Crutzen, P. J.: Modeling halogen chemistry in the marine boundary layer 1. Cloud-free MBL, J. Geophys. Res., 107, D174341, doi:10.1029/2001JD000942, 2002.

von Glasow, R., von Kuhlmann, R., Lawrence, M. G., Platt, U., and Crutzen, P. J.: Impact of reactive bromine chemistry in the troposphere, Atmos. Chem. Phys., 4, 2481–2497, doi:10.5194/acp-4-2481-2004, 2004.

Wachsmuth, M., Gäggeler, H. W., von Glasow, R., and Ammann, M.: Accommodation coefficient of HOBr on deliquescent sodium bromide aerosol particles, Atmos. Chem. Phys., 2, 121–131, doi:10.5194/acp-2-121-2002, 2002.

Wang, T. X. and Margarem, D. W.: Kinetics of reversible chlorine hydrolysis: temperature dependence and general-acid/base-assisted mechanisms, Inorg. Chem., 33, 1050–1055, 1994.

Wexler, A. S. and Clegg, S. L.: Atmospheric aerosol models for systems including the ions H^+, NH_4^+, Na^+, SO_4^{2-}, NO_3^-, Cl^-, Br^- and H_2O, J. Geophys. Res., 107, 4207–4220, 2002.

Wilson, T. R. S.: Salinity and the major elements of sea water, in: Chemical Oceanography, 1st, 2nd edn., edited by: Riley, J. P. and Skirrow, G., Academic, Orlando, FL, 365–413, 1975.

Yang, X., Cox, R. A., Warwick, N. J., Pyle, J. A., Carver, G. D., O'Connor, F. M., and Savage, N. H.: Tropospheric bromine chemistry and its impacts on ozone: a model study, J. Geophys. Res., 110, D23311, doi:10.1029/2005JD006244, 2005.

Table 1. Summary of experimental data reported on HOBr uptake coefficient and $HOBr_{(aq)}$ reaction kinetics under tropospheric conditions.

Aerosol or Solution	Temperature K	k_{ter} $M^{-2}\,s^{-1}$	k^{I} s^{-1}	k^{II} $M^{-1}\,s^{-1}$	γ_{HOBr}	α_{HOBr}	Ref.
$HOBr + Cl^{-}_{(aq)}$							
HCl-acidifed NaCl aerosol with HCl : NaCl = 0.1 : 1	298	–	–	–	> 0.2	–	a
H_2SO_4-acidified sea-salt aerosol with H_2SO_4 : NaCl = 1.45 : 1	296	–	10^3	–	10^{-3}–10^{-2}	–	b
$BrCl_{(aq)}$ solution, pH = 6.4	298	2.3×10^{10}	–	–	–	–	c
$HOBr + Br^{-}_{(aq)}$							
HOBr uptake onto supersaturated $NaBr_{(aq)}$, $Br^{-}_{(aq)} > 0.2\,M$, at very low $[HOBr_{(g)}]$	296 ± 2	–	–	–	–	0.6	d
$Br_{2\,(aq)}$ solution, pH = 2.7–3.8	298	1.6×10^{10}	–	–	–	–	e
$Br_{2\,(aq)}$ solution, pH = 1.9–2.4	298	$1.6(\pm 0.2) \times 10^{10}$	–	–	–	–	f

[a] Abbatt and Waschewsky (1998)
[b] Pratte and Rossi (2006)
[c] Liu and Margarem (2002)
[d] Wachsmuth et al. (2002)
[e] Eigen and Kustin (1962)
[f] Beckwith et al. (1996)

Table 2. Extraction of second-order rate constant values, k^{II} from reported experimental data. For HOBr+Br, k^{II} is derived from reported termolecular rate constants using $k^{\mathrm{II}} = k_{\mathrm{ter}} \cdot [\mathrm{H}^+_{(aq)}]$. For HOBr + Cl^- k^{II} is derived from a reported termolecular rate constant using $k^{\mathrm{II}} = k_{\mathrm{ter}} \cdot [\mathrm{H}^+_{(aq)}]$ and from reported first-order rate constant data, k^{I} using $k^{\mathrm{II}} = k^{\mathrm{I}}/[\mathrm{Cl}^-_{(aq)}]$. Molarity and activity of $\mathrm{Cl}^-_{(aq)}$ and $\mathrm{H}^+_{(aq)}$ were calculated using the E-AIM model at 298.15 K. See Methods.

Experiment	T K	RH %	wt% H_2SO_4	pH	$\mathrm{Cl}^-_{(aq)}$ Activity M	k_{ter} $M^{-2}\,s^{-1}$	k^{I} s^{-1}		k^{II} $M^{-1}\,s^{-1}$		Ref.
HOBr + Br^-											
$Br_{2\,(aq)}$	293	–	–	2.7–3.6	–	1.6×10^{10}	–		4×10^6–3.2×10^7		a
$Br_{2\,(aq)}$	298	–	–	1.9–2.4	–	$1.6\ (\pm 0.2) \times 10^{10}$	–		6.1×10^7–1.9×10^8		b
HOBr+Cl^-											
$BrCl_{(aq)}$	298	–	–	6.4	2.0	2.3×10^{10}	–		8.8×10^3		c
							($\alpha = 0.2^*$)	($\alpha = 0.02^*$)	($\alpha = 0.2^*$)	($\alpha = 0.02^*$)	
H_2SO_4 : NaCl (1.45 : 1)	296	77	31.7	−0.84	0.056		922	1855	1.6×10^4	3.3×10^4	d
	296	79	30.00	−0.75	0.069		1050	2510	1.5×10^4	3.6×10^4	
	296	80	29.1	−0.71	0.076		1140	3010	1.5×10^4	3.9×10^4	
	296	85	24.2	−0.48	0.127		800	1485	6.3×10^3	1.2×10^4	
	296	90	17.7	−0.21	0.209		995	2355	4.8×10^3	1.1×10^4	
H_2SO_4 : NaCl (1.45 : 1) NSS	296	77	31.7	−0.84	0.056		1960	44 000	3.5×10^4	7.8×10^5	d
H_2SO_4 : NaCl (1.45 : 1) RSS	296	77	31.7	−0.84	0.056		545	795	9.6×10^3	1.4×10^4	d
	296	79	30.00	−0.75	0.069		720	1225	1.0×10^4	1.8×10^4	
	296	80	29.1	−0.71	0.076		1090	2600	1.4×10^4	3.4×10^4	
	296	85	24.2	−0.48	0.127		815	1580	6.4×10^3	1.2×10^4	
	296	90	17.7	−0.21	0.209		710	1210	3.4×10^3	5.8×10^3	

[a] Termolecular rate constant reported by Eigen and Kustin (1962).

[b] Termolecular rate constant reported by Beckwith et al. (1996).

[c] Termolecular rate constant reported by Liu and Magarem (2001) for buffered aerosol containing $\mathrm{Cl}^-_{(aq)}$ at pH = 6.4 at T = 298 K.

[d] First-order rate constant, $k^{\mathrm{I}}_{\mathrm{rxn}}$ data reported by Pratte and Rossi (2005) for aerosol mixture at H2SO4:NaCl = 1.45, for laboratory sea-salt, natural sea-salt (nss) or recrystalised sea-salt (rss). Pratte and Rossi (2006) assumed two different accommodation coefficients (α = 0.2, α = 0.02) in the derivation of $k^{\mathrm{I}}_{\mathrm{rxn}}$ values from their uptake experiments, the former being closest to α = 0.6 reported on $\mathrm{NaBr}_{(aq)}$ aerosol by Wachsmuth et al. (2002).

Table 3. Underlying rate constant data (k_1, k_{-1}, k_0 k_H) used in k^{II} parameterisations of Fig. 1.

	HOBr + Br	HOBr + Cl
k_1, M^{-1} s^{-1}	$5\times10^{8\,b,a}$	$1.2\times10^{4\,c}$
k_{-1}, s^{-1}	$5\times10^{8\,b,a}$	$1.1\times10^{4\,c}$
k_0, s^{-1}	$10^{4\,a}$	$2\times10^{1\,c}$
k_H, M^{-1} s^{-1}	$2\times10^{10\,a}$	$2\times10^{10\,c}$

[a] estimated in this study, [b] derived from Eigen and Kustin (1962), [c] derived from Kumar and Margerum (1987).

Table 4. Predicted uptake coefficients compared to reported uptake on experimental aerosol. [a] Br^- concentration prior to aerosol dehumidifying (reported reduction in volume during dehumidifying indicates actual concentration may be a factor of ~ 3 higher). [b] modal radius, although particles > 0.2 µm exist within the reported size spectrum.

Experimental aerosol:	NaBr aerosol (Wachsmuth et al., 2002) supersaturated $NaBr_{(aq)}$	HCl-acidified NaCl aerosol (Abbatt and Waschewsky, 1998) HCl/NaCl = 0.1 : 1	H_2SO_4-acidified sea-salt aerosol (Pratte and Rossi, 2006) H_2SO_4/NaCl = 1.45 : 1	
γ_{HOBr}: observed	0.6 ± 0.2	> 0.2	$(0.1–0.3) \times 10^{-2}$ at RH 40 to 70 %	$(1.0 \pm 0.2) \times 10^{-2}$ at RH ≥ 76 %
Uptake Model Parameters:				
Temperature	298.15	298.15	298.15	298.15
α (accommodation coefficient)	0.6	0.6	0.6	0.6
Na concentration ($\mu mol\,m^{-3}$)	–	0.2	0.8	0.8
RH, %	80	76	50	80
$[Br^-_{(aq)}]$, M	> 0.2[a]	–	–	–
$[Cl^-_{(aq)}]$, M (E-AIM)	–	6.6	4.4×10^{-3}	7.6×10^{-2}
$[H^+_{(aq)}]$, M (E-AIM)	$\sim 2 \cdot 10^{-6}$	2.3	83	5
pH	~ 6	−0.3	−1.9	−0.7
k^{II}, $M^{-1}\,s^{-1}$	3×10^4	10^4	10^4	10^4
k_{ter}, $M^{-2}\,s^{-1}$	1.6×10^{10}	2.3×10^{10}	2.3×10^{10}	2.3×10^{10}
Particle radius, µm	> 0.03[b]	1.0	~ 0.17	~ 0.17
wt% H_2SO_4	–	–	48	29
HOBr solubility, $M\,atm^{-1}$	6.1×10^3	6.1×10^3	364	364
HOBr Diffusion constant, $cm^2\,s^{-1}$	1.42×10^{-5}	1.42×10^{-5}	5.5×10^{-6}	1.0×10^{-5}
γ_{HOBr}: old approach (where $k^I = k_{ter} \cdot [X^-_{(aq)}] \cdot [H^+_{(aq)}]$)	$0.1 < \gamma_{HOBr} \leq 0.6$	0.6	0.6	0.6
γ_{HOBr}: new approach (where $k^I = k^{II} \cdot [X^-_{(aq)}]$)	$0.1 < \gamma_{HOBr} \leq 0.6$	0.6	2×10^{-4}	7×10^{-3}

Title Page
Abstract | Introduction
Conclusions | References
Tables | Figures
◀| |▶
◀ ▶
Back | Close
Full Screen / Esc
Printer-friendly Version
Interactive Discussion

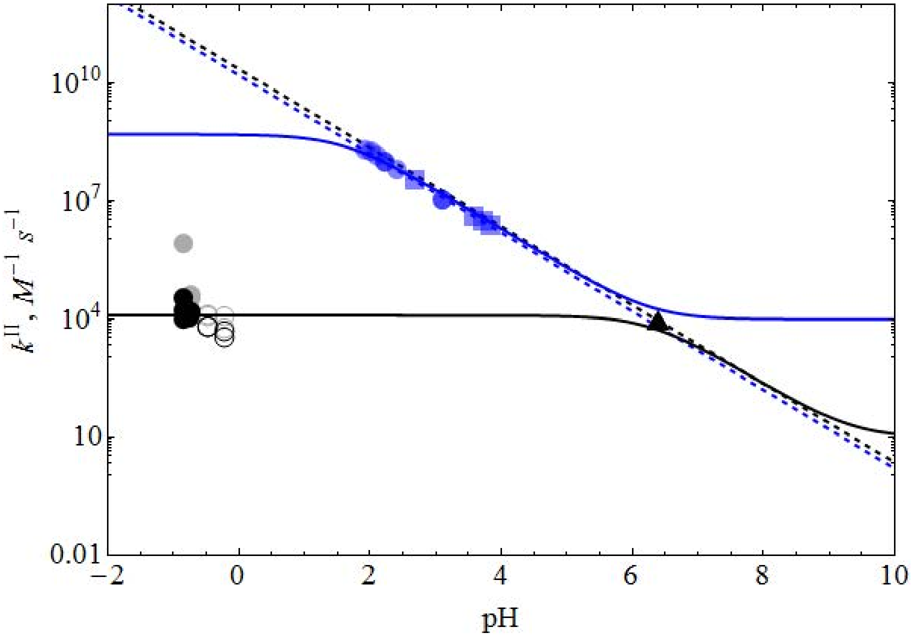

Fig. 1. Second order rate constants for the reaction of HOBr with Br^- and Cl^- as a function of pH. Experimental estimates for k^{II} for $\mathrm{HOBr} + \mathrm{Br}^-$ derived from data from Eigen and Kustin (1962) and Beckwith et al. (1996), (blue squares and circles respectively) shown alongside model estimate (blue line) according to the acid-assisted mechanism The blue dotted line denotes the rate constant assuming termolecular kinetics across all pH. Experimental estimates for k^{II} for $\mathrm{HOBr} + \mathrm{Cl}^-$ derived from data from Liu and Margarem (2001) at pH = 6.4 (black triangle) and Pratte and Rossi (2006) at pH −1 to 0 (black and grey disks for data at RH = 77–80 %, open circles for RH = 85–90 %), are shown alongside model estimate (black line) according to the general acid-assisted mechanism. The black dotted line denotes k^{II} predicted using the three body approach that assumes termolecular kinetics across all pH.

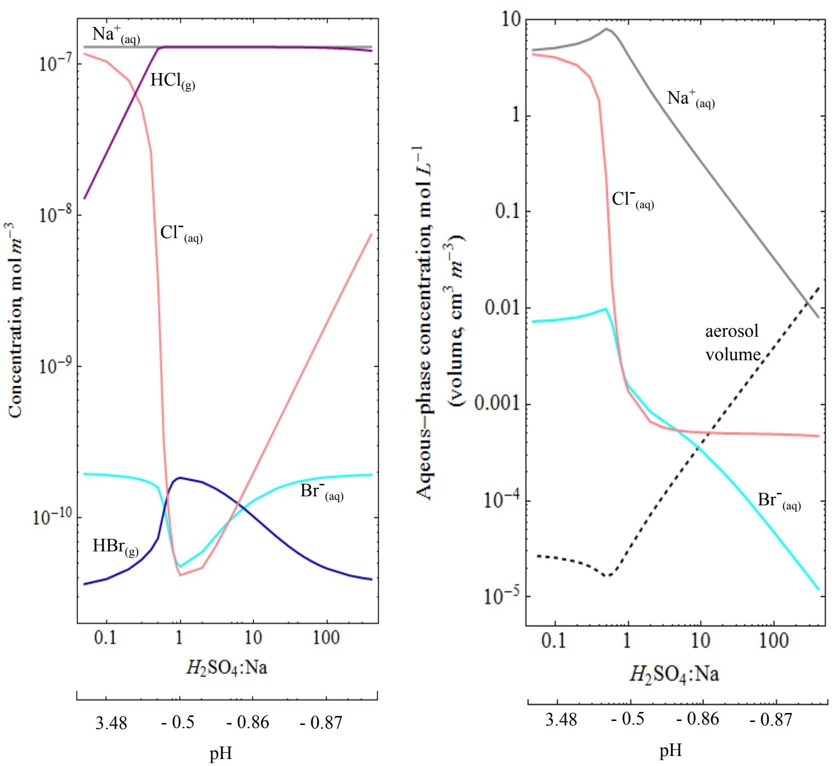

Fig. 2. Gas-aerosol partitioning according to E-AIM thermodynamic model III for a progressively H_2SO_4-acidified model sea-salt aerosol. Temperature is 298 K, relative humidity is 80 %. Na concentration was set to 1.3×10^{-7} mol m^{-3}, equivalent to a marine environment PM_{10} of 10 µg m^{-3} (Seinfeld and Pandis, 2006) assuming $NaCl_{(aq)}$. Molar concentrations (mol m^{-3}) of Na^+ (gray), $HCl_{(g)}$ (purple), $Cl^-_{(aq)}$ (pink), $Br^-_{(aq)}$ (light blue), $HBr_{(g)}$ (dark blue) are shown as well as aqueous-phase concentration (mol L^{-1}) as a function of H_2SO_4 : Na for $Cl^-_{(aq)}$ (pink), $Br^-_{(aq)}$ (light blue), and $Na^+_{(aq)}$ (grey). Aerosol volume (cm^3 m^{-3}) is shown by black dotted line.

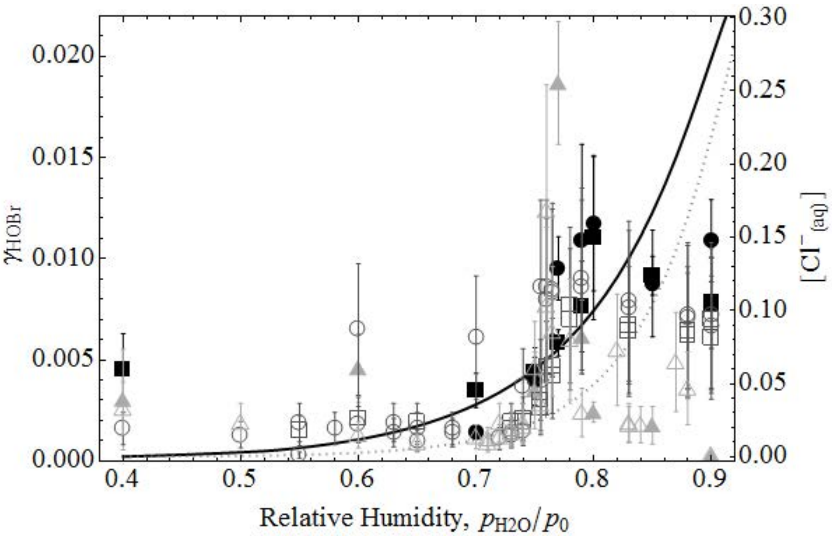

Fig. 3. Dependence of reactive uptake coefficient for HOBr on relative humidity (RH) in the experiments of Pratte and Rossi (2006) on H_2SO_4-acidified sea-salt aerosol (H_2SO_4 : NaCl = 1.45 : 1) at 296 K, on acidified sea-salt (circles), recrystallized sea-salt (squares) and natural sea-salt (triangles), under two experimental set-ups: (i) the observed rate of $HOBr_{(g)}$ decay for a measured aerosol size distribution, with effective radius ranging over 165–183 nm (filled shapes), and (ii) a survey type mode with HOBr depletion monitored as a function of RH (unfilled shapes, with reported error estimated at 30–50 %) over a constant reaction time. The modelled uptake coefficient for HOBr (black line) was calculated for particles with 170 nm effective radius at the experimental temperature of 296 K, and an aerosol mixture of H_2SO_4 : NaCl ratio 1.45 : 1. Within the uptake calculation, $k^I = k^{II}\,[Cl^-_{(aq)}]$ where k^{II} is according to the new parameterisation (Fig. 1) and $Cl^-_{(aq)}$ molarity (dotted line) and activity coefficients were calculated using the E-AIM thermodynamic model at 298 K. The model and experimental uptake coefficients show some agreement in terms of magnitude and trend with RH. In contrast, uptake calculations based on the termolecular approach that yield $\gamma \sim 0.6$ across all RH (not shown).

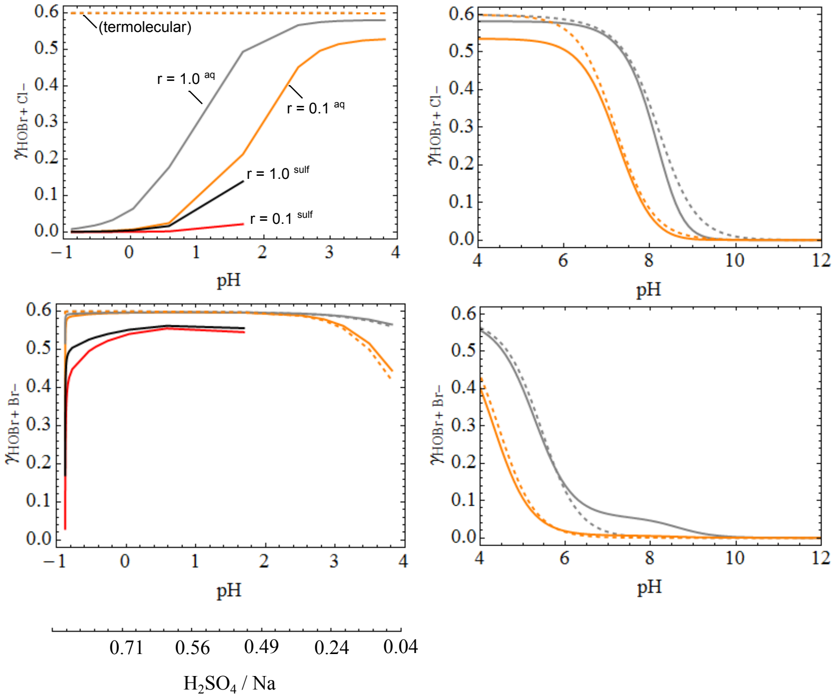

Fig. 4. Variation in the HOBr uptake coefficient with pH, for reaction of HOBr with (upper) Cl^- and (lower) Br^- on H_2SO_4-acidified sea-salt aerosol. Gray and orange lines denote uptake onto 1 and 0.1 µm radius particles, respectively. Black and red lines denote uptake onto 1 and 0.1 µm radius particles calculated using H^* and D_l parameterisations for HOBr reactive uptake into sulfuric acid (rather than water), shown only for H_2SO_4 : Na ratios greater than 0.5. Relative humidity is set to 80 % and Na concentration 1.3×10^{-7} mol m^{-3} (equivalent to a PM_{10} of 10 µg m^{-3} in the marine environment, Seinfeld and Pandis, 2006). Our new calculations show the HOBr reactive uptake coefficients decline at high acidity, in contrast to uptake coefficient calculations assuming termolecular kinetics (dashed lines).

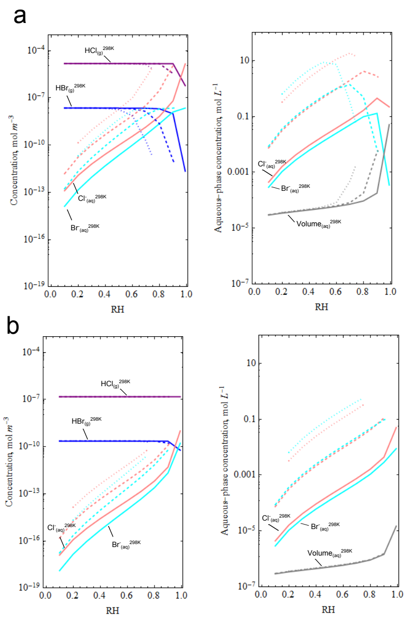

Fig. 5. Predicted volcanic plume composition for **(a)** strong plume (30 µmol m^{-1}, corresponding to 1 ppmv SO_2 at 4 km in a standard atmosphere) and **(b)** weak plume (0.3 µmol m^{-1}, corresponding to 0.01 ppmv SO_2) strengths. Gas-aerosol partitioning predicted according to E-AIM thermodynamic model I for a volcanic plume that has molar composition $(SO_2) : HCl : HBr : SO_4^{2-} = (1) : 0.5 : 0.00075 : 0.01$, representing a typical Arc volcano emission such as Etna. Plume halogen composition (in mol m^{-3} of atmosphere) and aqueous-phase composition (in mol L^{-1}) are shown as a function of RH, and for three different temperatures: 293, 263 and 243 K (thick, dashed and dotted lines, respectively), for conditions where aerosol is predicted to be purely in liquid form. Concentrations of $HCl_{(g)}$ (purple), $HBr_{(g)}$ (blue), $Cl^-_{(aq)}$ (pink), $Br^-_{(aq)}$ (cyan) with aqueous phase volume density (cm^3 m^{-3}, grey lines). For clarity, only 298 K model output is labelled.

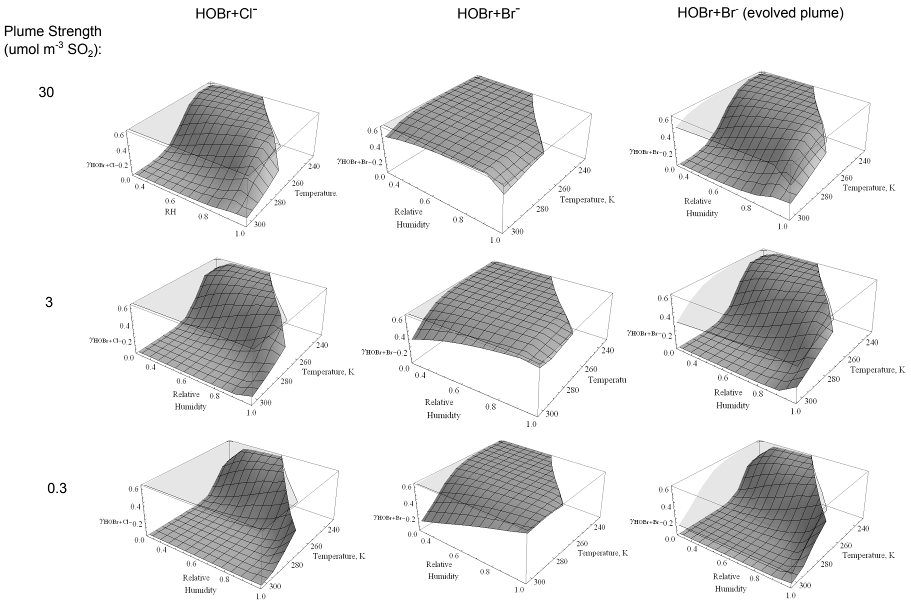

Fig. 6. HOBr + Cl^- and HOBr + Br^- reactive uptake coefficients onto volcanic sulphate aerosol particles of 1 µm radius, calculated using our revised HOBr kinetics. Calculations are performed for a typical Arc or subduction zone volcanic plume composition containing a (SO_2) : HCl : H_2SO_4 : HBr molar ratio mixture of 1 : 0.5 : 0.01 : 0.00075. The plume strength is 30, 3 or 0.3 $\mu mol\,m^{-3}$, equivalent to approximately 1, 0.1, 0.01 ppmv SO_2 at 4 km altitude (US standard atmosphere). Also shown is the HOBr + Br^- uptake coefficient for an evolved plume where significant BrO chemistry is underway, and it is assumed Br- concentrations have become depleted to the level: $[Br^-_{(aq)}] = 1.3/(1.8 \times 10^4) = 7 \times 10^{-5} \cdot [Cl^-_{(aq)}]$. For comparison, uptake coefficients calculated using the termolecular approach, are shown (light grey) to yield higher values across all parameter space, typically accommodation-limited.